

**TAYLOR-COUETTE INSTABILITY OF A BINGHAM FLUID**

by

MARIA PAULINA LANDRY

BMath (Applied Mathematics, Honours Co-op) University of Waterloo, 2001

A THESIS SUBMITTED IN PARTIAL FULFILLMENT OF

THE REQUIREMENTS FOR THE DEGREE OF

MASTER OF SCIENCE

in

THE FACULTY OF GRADUATE STUDIES

Department of Mathematics

We accept this thesis as conforming  
to the required standard

THE UNIVERSITY OF BRITISH COLUMBIA

December 2003

© Maria Paulina Landry, 2003

In presenting this thesis in partial fulfillment of the requirements for an advanced degree at the University of British Columbia, I agree that the Library shall make it freely available for reference and study. I further agree that permission for extensive copying of this thesis for scholarly purposes may be granted by the head of my department or by his or her representatives. It is understood that copying or publication of this thesis for financial gain shall not be allowed without my written permission.

Department of Mathematics  
The University of British Columbia  
Vancouver, Canada

Date Dec. 16, 2003

# Abstract

Stability of a Bingham fluid in Taylor-Couette flow is studied. Of interest is to determine the critical values of the inner and outer cylinder angular velocities which cause the linear instability in the system. We introduce a perturbation into the basic flow, and examine the linearized Navier-Stokes equations for the perturbation. Assuming a normal mode solution for the perturbation, we obtain an eigenvalue problem which determines when the perturbation will grow or decay with time. In the case of a plug region at the outer cylinder wall, additional boundary conditions are applied at the yield surface. The marginal stability curve is generated numerically using a finite difference method. In addition to numerical analysis, heuristic arguments and energy methods are applied to find a lower bound for stability.

# Table of Contents

<b>Abstract</b>	<b>ii</b>
<b>Table of Contents</b>	<b>iii</b>
<b>List of Tables</b>	<b>v</b>
<b>List of Figures</b>	<b>vi</b>
<b>Acknowledgement</b>	<b>vii</b>
<b>Chapter 1. Introduction</b>	<b>1</b>
1.1 Historical Perspective of the Taylor-Couette Problem .....	2
1.2 Bingham Fluids and the Taylor-Couette Problem .....	3
1.2.1 Applications .....	4
1.2.2 Previous Work .....	6
1.3 Thesis Outline .....	6
<b>Chapter 2. Governing Equations</b>	<b>8</b>
2.1 Basic Solutions .....	8
2.2 Dimensionless Parameters .....	10
2.3 The Velocity Profile .....	11
2.4 Relation Between $\tau_i$ and $\Omega$ .....	14
2.4.1 Region I .....	14
2.4.2 Region II .....	15
2.5 Visualizing Regions I, II and III .....	16
2.6 Limit as $B \rightarrow 0$ .....	17
<b>Chapter 3. Linear Stability Analysis</b>	<b>20</b>
3.1 Linear Perturbation Equations .....	20
3.2 The Method of Normal Modes .....	25
3.3 Boundary Conditions for the Perturbation .....	27
3.3.1 Region I: No Plug .....	27
3.3.2 Region II: Plug on the Wall .....	28
<b>Chapter 4. Axisymmetric Disturbance</b>	<b>31</b>
4.1 Axisymmetric Equations .....	31
4.2 Numerical Methods .....	34
4.2.1 Basic Flow Equations .....	35
4.2.2 Finite Difference Method .....	35
4.2.3 Finding the Critical $Re_1$ .....	35
<b>Chapter 5. Results for an Axisymmetric Disturbance</b>	<b>39</b>
5.1 Numerical Results .....	39

*Table of Contents*

5.1.1	Comparison with Newtonian Results .....	39
5.1.2	Results for $B > 0$ .....	39
5.2	Heuristic Results .....	43
5.3	A Lower Bound for Stability .....	47
5.3.1	Simplifying the Integrals .....	50
5.3.2	Bounding the Integrals .....	53
5.3.3	Applying the Poincaré Inequality .....	56
5.3.4	Results .....	57
<b>Chapter 6. Conclusions</b>		<b>59</b>
<b>Bibliography</b>		<b>60</b>
<b>Appendix A. Numerical Approximations of the Eigenvalue Problem</b>		<b>61</b>

# List of Tables

5.1	Approximate least squares values for $a$ and $q$ for $B \geq 200$ with $N = 50$ . . . . .	43
-----	---	----

# List of Figures

1.1	Taylor-vortex flow of a Newtonian fluid [10]. . . . .	2
1.2	Regions observed for the Taylor-Couette flow of a Newtonian with $\hat{R}_1/\hat{R}_2 = 0.883$ , Andereck et al [1]. . . . .	3
2.1	Regions with $\eta = 0.883$ for various values of $B$ . Region III is the line $Re_1 = \eta Re_2$ . . .	18
2.2	Regions with $B = 5$ for various values of $\eta$ . . . . .	18
4.1	$Re_1$ is too small. Instability has not yet occurred. . . . .	36
4.2	$Re_1$ is too large. Instability has already occurred. . . . .	37
4.3	$Re_1 = Re_{1crit}$ . . . . .	37
4.4	Marginal stability curve for $B = 10$ , $\eta = 0.883$ . . . . .	38
4.5	Flowchart of marginal stability code . . . . .	38
5.1	Comparison of our numerical calculations against data from [1] for $m = 0$ . . . . .	40
5.2	Marginal stability curves versus regions for $\eta = 0.883$ with $N = 50$ . . . . .	40
5.3	Marginal stability curves $\eta = 0.883$ and varying $B$ . . . . .	41
5.4	$Re_{1crit}$ becomes progressively independent of $Re_2$ as $B$ increases. . . . .	42
5.5	$Re_{1crit}$ for $B = 1000$ with the asymptotic solution $Re_{1crit} = aB^q$ ; $a = e^{4.0467}$ , $q = 1.2169$ . . . . .	42
5.6	For a larger gap, $Re_{1crit}$ is not necessarily an increasing function of $B$ . . . . .	44
5.7	Marginal stability curves with $\eta = 0.5$ and varying $B$ . . . . .	44
5.8	Marginal stability curve for a Newtonian fluid along with the Rayleigh criterion. . . .	46
5.9	Solid lines: Rayleigh criterion. Dashed line: Rigid rotation $Re_1 = \eta Re_2$ ; $\eta = 0.883$ . . . .	48
5.10	Solid line: $f(Re_1, Re_2) = 0$ . Dashed line: Rigid rotation $Re_1 = \eta Re_2$ ; $\eta = 0.883$ . . . .	58

# Acknowledgement

This thesis was conducted under the supervision of Dr. Ian Frigaard and Dr. Mark Martinez. I would like to thank them for their guidance, insight and encouragement throughout. I would like to acknowledge the help of Dr. Randall Tagg from the University of Colorado who provided data for this thesis.

For funding this research, I would also like to thank the Advanced Systems Institute of British Columbia and Metso Corporation.

# Chapter 1

## Introduction

We will consider the stability of a Bingham fluid between two infinitely long concentric cylinders with inner and outer radii  $\hat{R}_1$  and  $\hat{R}_2$  respectively. Both the inner and outer cylinders rotate independently at respective angular speeds  $\hat{\Omega}_1$  and  $\hat{\Omega}_2$ . The Taylor-Couette problem is the study of the flow behaviour between the cylinders. For sufficiently small values of the angular speeds, Couette flow is observed; a laminar azimuthal shear flow between these two concentric cylinders.

For Newtonian flow, the angular speeds can be increased so that a critical flow state is obtained and the particles travel in helical paths, where the vortices are layered one on top of the other as seen in figure 1.1. These helical vortices are known as Taylor vortices and this primary instability is known as Taylor-vortex flow. Taylor-vortex flow is, however, a stable flow and further instabilities can be reached by increasing the angular speeds. Observe that this linear instability is axisymmetric and periodic. Furthermore, note that the Taylor-Couette flow demonstrates the non-uniqueness of the Navier-Stokes equations, since there are at least two flows which mathematically satisfy these equations with the same boundary conditions: the laminar flow and the perturbed flow.

We would like to determine the critical values of  $\hat{\Omega}_1$  and  $\hat{\Omega}_2$  for instability of a Bingham fluid. In the sections to follow, we will describe in detail the properties of a Bingham fluid and how the study of Taylor-Couette flow of a Bingham fluid differs from the study of Taylor-Couette flow of a Newtonian fluid.

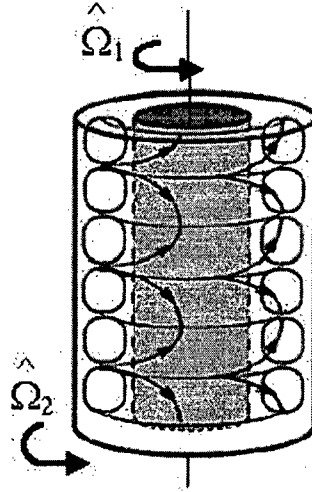


Figure 1.1: Taylor-vortex flow of a Newtonian fluid [10].

## 1.1 Historical Perspective of the Taylor-Couette Problem

In 1923, G.I. Taylor [11] was the first to predict analytically, and support experimentally, the occurrence of Taylor vortices with a Newtonian fluid. He assumed an axisymmetric disturbance, and a narrow gap between the cylinders. Since then, there have been many papers written on the Taylor-Couette problem. The literature review by Tagg [10] is a plentiful source for references, methods of approach to the Taylor-Couette problem of a Newtonian fluid, and results obtained.

An extensive study by Andereck, Liu and Swinney [1] shows regimes observed for various angular speeds as seen in figure 1.2. In this figure,  $Re_1$  and  $Re_2$  are the inner and outer cylinder Reynolds numbers respectively (see section 2.2), and the radius ratio is fixed at  $\eta = \hat{R}_1/\hat{R}_2 = 0.883$ . The transition from Couette to Taylor-vortex flow is observed to be the primary instability. Flow regions beyond the primary instability are shown as well. Of interest in this thesis is to produce the linear instability curve in the  $(Re_2, Re_1)$ -plane when the fluid is a Bingham fluid.

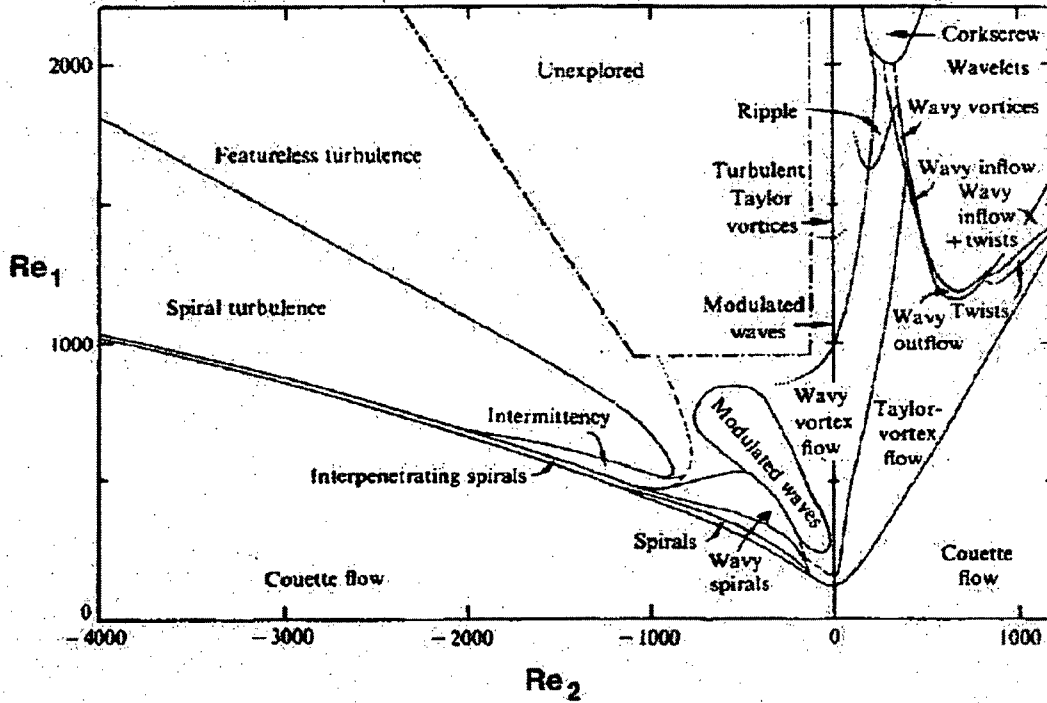


Figure 1.2: Regions observed for the Taylor-Couette flow of a Newtonian with  $\hat{R}_1/\hat{R}_2 = 0.883$ , Andereck et al [1].

## 1.2 Bingham Fluids and the Taylor-Couette Problem

Unlike a Newtonian fluid, a viscoplastic fluid is a fluid with a yield stress. That is, the yield stress needs to be exceeded in order for the fluid to flow. Wherever the stress does not exceed the yield stress, there is no flow and this region is called the unyielded region. The region where there is flow is called the yielded region. Viscoplastic fluids can be modeled by one of the Bingham, Casson, or Herschel-Bulkley equations which all provide mathematical relations between the stress and strain-rate. The most widely used model, because of its simplicity, is the Bingham fluid model [2], where the stress/strain-rate relation is given by

$$\hat{\tau}_{ij} = \left( \hat{\mu}_p + \frac{\hat{\tau}_y}{\hat{\gamma}} \right) \hat{\gamma}_{ij} \iff \hat{\tau} > \hat{\tau}_y$$

$$\hat{\gamma} = 0 \iff \hat{\tau} \leq \hat{\tau}_y$$

where  $\hat{\tau}_{ij}$  and  $\hat{\gamma}_{ij}$  are the deviatoric stress and rate of strain tensors respectively,

$$\hat{\tau} = \left( \frac{1}{2} \hat{\tau}_{ij} \hat{\tau}_{ij} \right)^{\frac{1}{2}}$$

is the second invariant of the deviatoric stress tensor and

$$\hat{\gamma} = \left( \frac{1}{2} \hat{\gamma}_{ij} \hat{\gamma}_{ij} \right)^{\frac{1}{2}}$$

is the second invariant of the rate of strain tensor. Here  $\hat{\mu}_p$  is the plastic viscosity and  $\hat{\tau}_y$  is the yield stress. In contrast, the stress/strain-rate relation for a Newtonian fluid with viscosity  $\hat{\mu}$  is given by

$$\hat{\tau}_{ij} = \hat{\mu} \hat{\gamma}_{ij}.$$

Note that once the yield stress is exceeded, the stress varies linearly with the strain rate as does that of a Newtonian fluid. In regions where the yield stress is not exceeded, the fluid moves as if it were a solid. The region where the fluid moves in rigid motion is called a plug region. In the case of a plug, additional boundary conditions are required at the yield surface.

For the Taylor-Couette flow of a Bingham fluid, we find that there are three basic types of flow:

I. No plug flow, II. Plug attached to the wall, and III. Rigid body rotation.

Examples of fluids with a yield stress include: pulp slurries, sewage sludge, drilling muds, unhardened cement, toothpaste and paint.

### 1.2.1 Applications

**Pulp suspensions:** Pulp suspensions are known to exhibit a yield stress. To the lowest order of approximation, we can approximate a pulp suspension with a Bingham fluid model.

Papermaking fibre suspensions are a mixture of wood fibre, water and clay as well as small quantities of inorganic salts and polymeric additives. This physical makeup leads to complex

rheological behaviour with the suspensions showing non-linear stress-strain relationships. The major feature of the stress-strain relationship is that of a non-Newtonian fluid.

It is widely known that pulp suspensions do not flow until a certain critical stress (or yield stress) is exceeded. Suspension yield stresses have been either measured directly using viscometers or inferred from dynamic and tensile measurements. For pulp suspensions, the yield stress has been typically correlated with the suspension mass concentration using equations of the form

$$\hat{\tau}_y = a(c_m - c_s)^b$$

where  $c_m$  is the mass concentration and  $c_s$  is the gel concentration. The parameters  $a$  and  $b$  depend upon the test procedure employed, the pulp type, and the degree of treatment. Values of  $b$  have been reported to range between 1.25 to 3.

With flowing papermaking suspensions, most experimental data relating the transition from a plug-like to a well-mixed state and then turbulent flow has been observed in pipe flows. The onset of drag reduction, observed to occur in the well-mixed state, has been characterized by criteria based upon power dissipation per unit volume. There has been very little work regarding transition in a rotating device, i.e. a pressure screen. The information generated in this thesis will help address this issue.

**Electrorheological (ER) fluids:** ER fluids are suspensions of dielectric particles in a non-conducting liquid. The primary effect of an electric field is to create a yield stress in the fluid. Typically, this can increase up to 5 kilopascals in the order of a millisecond. Papers such as [5] use the Bingham model to model the flow of an ER fluid. There are many technological applications including shock absorbers and electronically controlled clutches. Often in these applications, the ER fluid serves as a hydraulic lubricant where the ER device involves rotational shear. The Taylor-Couette flow is an archetypical flow and can be used to model instabilities in these applications. For safety concerns, it is important to determine when such instability would occur.

### 1.2.2 Previous Work

Linear stability of Taylor-Couette flow of a Bingham fluid has been studied by Graebel [8] who generalized the methods of Chandrasekhar [3] by using a narrow gap approximation to analyze the stability of a Bingham fluid once the normal mode equations were obtained. In the case of a plug on the outer cylinder wall, the gap was considered to be the fluid region between the inner cylinder and the plug. Graebel concluded that the yield stress acts as a stabilizing agent in the flow.

Recent papers on linear stability of Poiseuille flow of a Bingham fluid, such as [6] and [7], present the approach which has been applied to Taylor-Couette flow in this thesis. Methods from [6] include linear stability analysis and applications of boundary conditions at the plug, which we follow in chapter 3. Furthermore, [7] provides a method for finding a conservative estimate for linear stability, which we apply in section 5.3.

### 1.3 Thesis Outline

Our objective is to determine when the linear instability of the Taylor-Couette flow of a Bingham fluid occurs. To do this, we will use linear stability analysis. In chapter 2, we first nondimensionalize all relevant parameters, and determine all the basic equations for the flow. Of importance are the dimensionless groups  $\eta$ ,  $Re_1$ ,  $Re_2$  and  $B$ , the Bingham number (see section 2.2), which determine all characteristics for the flow. By finding the stress at any point, we can determine where a plug region occurs. From this point, we obtain three basic types of flow: I. No plug flow, II. Plug on the wall, III. Rigid body rotation. Furthermore, a velocity profile is calculated for each of these flow types.

In chapter 3 we introduce a perturbation to the basic velocity profile, and study the motion of the perturbation by linearizing the Navier-stokes equations, and assuming a normal mode expansion for the perturbation. Furthermore, no-slip boundary conditions are applied at the cylinder walls and, in the case of type II flow, additional boundary conditions are applied at the yield surface.

## *Chapter 1. Introduction*

Since the linear instability for a Newtonian fluid has been observed to be axisymmetric, we focus our efforts on an axisymmetric disturbance in chapter 4. The normal mode approach leads to an eigenvalue problem for the growth rate of the perturbation. Depending on the sign of the real part of the eigenvalue, we can determine whether the perturbation grows or decays with time. We then describe the numerical methods used to solve this eigenvalue problem. Numerical results and analytical lower bounds are presented in chapter 5.

# Chapter 2

## Governing Equations

### 2.1 Basic Solutions

Consider the flow between two infinitely long concentric cylinders with inner radius  $\hat{R}_1$  and outer radius  $\hat{R}_2$ . The cylinders rotate independently with inner angular speed  $\hat{\Omega}_1$  and outer angular speed  $\hat{\Omega}_2$ . Let  $\hat{r}$ ,  $\theta$  and  $\hat{z}$  be the radial, azimuthal and axial directions of motion respectively. Assuming a velocity profile of the form  $\hat{\mathbf{U}} = \hat{V}(\hat{r})\mathbf{e}_\theta$  gives the stress/strain-rate relation

$$\hat{\tau}_{\hat{r}\theta} = \left( \hat{\mu}_p + \frac{\hat{\tau}_y}{\hat{\gamma}} \right) \hat{\gamma}_{\hat{r}\theta} \iff \hat{\tau} > \hat{\tau}_y \quad (2.1)$$

$$\hat{\gamma} = 0 \iff \hat{\tau} \leq \hat{\tau}_y \quad (2.2)$$

where  $\hat{\mu}_p$  is the plastic viscosity,  $\hat{\tau} = |\hat{\tau}_{\hat{r}\theta}|$  is the stress,  $\hat{\gamma} = |\hat{\gamma}_{\hat{r}\theta}|$  is the strain rate, and  $\hat{\tau}_y$  is the yield stress that needs to be exceeded in order for fluid to flow. All of the other stress components vanish. If the yield stress is not exceeded at a point, then the strain rate is zero at that point so that there is no relative motion between particles and the fluid moves as if it were a rigid body. For this reason, the region where  $\hat{\tau} \leq \hat{\tau}_y$  is called a **plug region**. The momentum equations are given by

$$\hat{r}: \quad \hat{\rho} \frac{\hat{V}^2}{\hat{r}} = \frac{\partial \hat{p}}{\partial \hat{r}} \quad (2.3)$$

$$\theta: \quad 0 = \frac{1}{\hat{r}^2} \frac{\partial}{\partial \hat{r}} (\hat{r}^2 \hat{\tau}_{\hat{r}\theta}). \quad (2.4)$$

There are two possible boundary conditions that can be applied to the inner cylinder. We can apply either an inner stress

$$\hat{\tau}_{\hat{r}\theta}(\hat{R}_1) = \hat{\tau}_i \quad (2.5)$$

or an inner velocity

$$\hat{V}(\hat{R}_1) = \hat{\Omega}_1 \hat{R}_1. \quad (2.6)$$

Looking at the  $\theta$ -momentum equation (2.4), we see that the former boundary condition is a more natural choice. Solving for  $\hat{\tau}_{\hat{r}\theta}$  in the  $\theta$ -momentum equation and applying the inner stress boundary condition gives

$$\hat{\tau}_{\hat{r}\theta} = \frac{\hat{R}_1^2 \hat{\tau}_i}{\hat{r}^2}. \quad (2.7)$$

We see that  $\hat{\tau}_{\hat{r}\theta}$  decreases as  $\hat{r}$  increases, therefore if a plug occurs in the flow it will be against the outer cylinder wall. If the stress at the outer cylinder is greater than the yield stress, then there will be no plug in the flow. If the stress at the inner cylinder is less than the yield stress, then the entire region between the cylinders will be a plug and the fluid will move in rigid body rotation. We obtain three basic solutions:

- |                          |   |
|--------------------------|---|
| I. No plug               | $\frac{ \hat{\tau}_i }{\hat{\tau}_y} > \left(\frac{\hat{R}_2}{\hat{R}_1}\right)^2$        |
| II. Partial plug         | $1 < \frac{ \hat{\tau}_i }{\hat{\tau}_y} \leq \left(\frac{\hat{R}_2}{\hat{R}_1}\right)^2$ |
| III. Solid body rotation | $\frac{ \hat{\tau}_i }{\hat{\tau}_y} \leq 1$  |

For each of regions I, II and III we need to apply the boundary condition

$$\hat{V}(\hat{R}_2) = \hat{\Omega}_2 \hat{R}_2. \quad (2.8)$$

Denote the location of the yield surface, or plug, by  $\hat{r} = \hat{R}_y$ . In case of a plug, we apply a third boundary condition

$$\hat{V}(\hat{R}_y) = \hat{\Omega}_2 \hat{R}_y. \quad (2.9)$$

## 2.2 Dimensionless Parameters

To nondimensionalize the problem, we will follow [4] by setting  $\mathbf{U} = \frac{1}{\hat{\Omega}_1 \hat{R}_1} \hat{\mathbf{U}}$ ,  $r = \frac{1}{\hat{d}} \hat{r}$ ,  $z = \frac{1}{\hat{d}} \hat{z}$ ,  $t = \frac{1}{\hat{T}} \hat{t}$ ,  $P = \frac{1}{\hat{P}_o} \hat{P}$ ,  $\tau = \frac{1}{\hat{\mu}_p} \hat{\tau}$  where  $\hat{d} = \hat{R}_2 - \hat{R}_1$ ,  $\hat{T} = \frac{\hat{\rho} \hat{d}^2}{\hat{\mu}_p}$  and  $\hat{P}_o = \frac{\hat{\mu}_p \hat{R}_1 \hat{\Omega}_1}{\hat{d}}$ . By convention, we take  $\hat{\Omega}_1 > 0$ . This nondimensionalization gives the rescaled Navier-Stokes equation

$$\mathbf{U}_t + Re_1(\mathbf{U} \cdot \nabla) \mathbf{U} = -\nabla P + \nabla \cdot \tau \quad (2.10)$$

where

$$Re_1 = \frac{\hat{\rho} \hat{R}_1 \hat{\Omega}_1 \hat{d}}{\hat{\mu}_p} \quad (2.11)$$

is the inner cylinder Reynolds number, and set

$$Re_2 = \frac{\hat{\rho} \hat{R}_2 \hat{\Omega}_2 \hat{d}}{\hat{\mu}_p} \quad (2.12)$$

as the outer cylinder Reynolds number. The stress/strain-rate relation is given by

$$\tau_{r\theta} = \left(1 + \frac{B}{\dot{\gamma}}\right) \dot{\gamma}_{r\theta} \iff \dot{\gamma} > B \quad (2.13)$$

$$\dot{\gamma} = 0 \iff \tau \leq B \quad (2.14)$$

where  $\dot{\gamma} = |\dot{\gamma}_{r\theta}|$  and  $\tau = |\tau_{r\theta}|$ . Here,

$$B = \frac{\hat{\tau}_y \hat{d}}{\hat{\mu}_p \hat{R}_1 \hat{\Omega}_1} \quad (2.15)$$

is the Bingham number which is the ratio of the yield stress to the viscous stress. If  $B = 0$ , then the fluid is Newtonian since no stress needs to be exceeded in order for the fluid to flow.

Let  $\eta = \hat{R}_1/\hat{R}_2$ . Then  $\hat{R}_1$  and  $\hat{R}_2$  get rescaled to

$$R_1 = \frac{\eta}{1 - \eta} \quad (2.16)$$

$$R_2 = \frac{1}{1 - \eta} \quad (2.17)$$

respectively. Note that with this rescaling, the gap width  $R_2 - R_1$  will always be 1. At the inner cylinder, we can apply either the inner stress boundary condition

$$\tau_{r\theta}(R_1) = \tau_i \quad (2.18)$$

or the inner velocity boundary condition

$$V(R_1) = 1. \quad (2.19)$$

If there is no plug, the outer cylinder boundary condition is given by

$$V(R_2) = \Omega \frac{R_2}{R_1} = \frac{\Omega}{\eta} \quad (2.20)$$

where  $\Omega = \hat{\Omega}_2/\hat{\Omega}_1$ . If we are in region II, then the boundary condition at the yield surface  $r = R_y$  is given by

$$V(R_y) = \Omega \frac{R_y}{R_1}. \quad (2.21)$$

## 2.3 The Velocity Profile

The rescaled stress is given by

$$\tau_{r\theta} = \frac{\tau_i R_1^2}{r^2} \quad (2.22)$$

and the three basic solutions are given by

- |                          |   |
|--------------------------|---|
| I. No plug               | $\frac{ \tau_i }{B} > \left(\frac{1}{\eta}\right)^2$        |
| II. Partial plug         | $1 < \frac{ \tau_i }{B} \leq \left(\frac{1}{\eta}\right)^2$ |
| III. Solid body rotation | $\frac{ \tau_i }{B} \leq 1$                                 |

If there is a plug (or unyielded region), the yield surface  $R_y$  occurs when  $|\tau_{r\theta}| = B$ . Therefore we solve the equation  $\left| \frac{\tau_i R_1^2}{R_y^2} \right| = B$  for  $R_y$  to obtain

$$R_y = \sqrt{\frac{|\tau_i|}{B}} R_1. \quad (2.23)$$

Note that in the yielded region,  $\tau_i > 0 \iff \tau_{r\theta} > 0 \iff \left(1 + \frac{B}{|\dot{\gamma}_{r\theta}|}\right) \dot{\gamma}_{r\theta} > 0 \iff \dot{\gamma}_{r\theta} > 0$ . Similarly,  $\tau_i < 0 \iff \dot{\gamma}_{r\theta} < 0$ , therefore, in the yielded region we have  $\text{sgn}(\dot{\gamma}_{r\theta}) = \text{sgn}(\tau_i)$ .

Using this result we obtain

$$\tau_{r\theta} = \dot{\gamma}_{r\theta} + B \text{sgn}(\dot{\gamma}_{r\theta}) = \dot{\gamma}_{r\theta} + B \text{sgn}(\tau_i). \quad (2.24)$$

We can rewrite  $\dot{\gamma}_{r\theta}$  as

$$\dot{\gamma}_{r\theta} = \tau_{r\theta} - B \text{sgn}(\tau_i) = \frac{\tau_i R_1^2}{r^2} - B \text{sgn}(\tau_i). \quad (2.25)$$

Using the above information and the fact that  $\dot{\gamma}_{r\theta} = \frac{dV}{dr} - \frac{V}{r} = r \frac{d}{dr} \left(\frac{V}{r}\right)$ , we obtain the differential equation

$$r \frac{d}{dr} \left(\frac{V}{r}\right) = \frac{\tau_i R_1^2}{r^2} - B \text{sgn}(\tau_i) \quad (2.26)$$

which gives

$$V = -\frac{1}{2} \frac{\tau_i R_1^2}{r} - rB \ln(r) \operatorname{sgn}(\tau_i) + Cr. \quad (2.27)$$

**Region I:** Apply the boundary condition  $V(R_2) = \Omega \frac{R_2}{R_1}$ .

$$\Omega \frac{R_2}{R_1} = -\frac{1}{2} \frac{\tau_i R_1^2}{R_2} - R_2 B \ln(R_2) \operatorname{sgn}(\tau_i) + CR_2$$

which gives

$$C = \frac{\Omega}{R_1} + \frac{1}{2} \frac{\tau_i R_1^2}{R_2^2} + B \ln(R_2) \operatorname{sgn}(\tau_i)$$

so that for  $R_1 \leq r \leq R_2$

$$V = \frac{\Omega}{R_1} r + \frac{1}{2} \tau_i R_1^2 r \left( \frac{1}{R_2^2} - \frac{1}{r^2} \right) + Br \ln \left( \frac{R_2}{r} \right) \operatorname{sgn}(\tau_i). \quad (2.28)$$

**Region II:** Applying the boundary condition  $V(R_y) = \Omega \frac{R_y}{R_1}$ , and using the fact that  $\dot{\gamma} = 0$  for  $R_y \leq r \leq R_2$  gives

$$V = \begin{cases} \frac{\Omega}{R_1} r + \frac{1}{2} \tau_i R_1^2 r \left( \frac{1}{R_y^2} - \frac{1}{r^2} \right) + Br \ln \left( \frac{R_y}{r} \right) \operatorname{sgn}(\tau_i) & \text{for } R_1 \leq r \leq R_y \\ \frac{\Omega}{R_1} r & \text{for } R_y \leq r \leq R_2 \end{cases} \quad (2.29)$$

**Region III:** We have that  $\dot{\gamma} = 0$  everywhere, so for  $R_1 \leq r \leq R_2$  we obtain

$$V = \frac{r}{R_1}. \quad (2.30)$$

We can express the velocity profile more concisely as

$$V = \begin{cases} \frac{\Omega}{R_1}r + \frac{1}{2}\tau_i R_1^2 r \left( \frac{1}{R_o^2} - \frac{1}{r^2} \right) + Br \ln \left( \frac{R_o}{r} \right) \operatorname{sgn}(\tau_i) & \text{for } R_1 \leq r \leq R_o \\ \frac{\Omega}{R_1}r & \text{for } R_o \leq r \leq R_2 \end{cases} \quad (2.31)$$

where  $R_o = \min\{R_y, R_2\}$ .

## 2.4 Relation Between $\tau_i$ and $\Omega$ .

Applying the boundary condition  $V(R_1) = 1$  to the velocity profile in the yielded region gives a relation between  $\tau_i$  and  $\Omega$ .

### 2.4.1 Region I

In region I we obtain the relation

$$\begin{aligned} 1 &= \Omega + \frac{1}{2}\tau_i R_1 \left( \frac{R_1^2}{R_2^2} - 1 \right) + BR_1 \ln \left( \frac{R_2}{R_1} \right) \operatorname{sgn}(\tau_i) \\ &= \Omega + \frac{1}{2}\tau_i R_1 (\eta^2 - 1) + BR_1 \ln \left( \frac{1}{\eta} \right) \operatorname{sgn}(\tau_i) \end{aligned} \quad (2.32)$$

which can be rearranged as

$$1 - \Omega = \frac{BR_1}{2} \left( \frac{|\tau_i|}{B} (\eta^2 - 1) + \ln \left( \frac{1}{\eta^2} \right) \right) \operatorname{sgn}(\tau_i). \quad (2.33)$$

Since we are in region I, we have  $\frac{|\tau_i|}{B} > \frac{1}{\eta^2}$ , therefore

$$\frac{|\tau_i|}{B} (\eta^2 - 1) + \ln \left( \frac{1}{\eta^2} \right) < \frac{\eta^2 - 1}{\eta^2} + \ln \left( \frac{1}{\eta^2} \right) = \ln \left( \frac{1}{\eta^2} \right) - \frac{1}{\eta^2} + 1 < 0 \quad (2.34)$$

for  $\eta < 1$ . Therefore, if  $\operatorname{sgn}(\tau_i) = -1$  then  $1 - \Omega > 0$  or  $\tau_i < 0 \Leftrightarrow \Omega < 1$ . Similarly,  $\tau_i > 0 \Leftrightarrow \Omega > 1$ . Therefore  $\operatorname{sgn}(\tau_i) = \operatorname{sgn}(\Omega - 1)$ , and can solve for  $\tau_i$  to obtain

$$\tau_i = \frac{2}{\eta^2 - 1} \left( \text{sgn}(\Omega - 1) B \ln(\eta) + (1 - \Omega) \left( \frac{1 - \eta}{\eta} \right) \right). \quad (2.35)$$

### 2.4.2 Region II

It is not possible to solve for  $\tau_i$  explicitly when we are working in region II. Applying  $V(R_1) = 1$  gives the relation

$$\begin{aligned} 1 &= \Omega + \frac{1}{2} \tau_i R_1^3 \left( \frac{1}{R_y^2} - \frac{1}{R_1^2} \right) + B R_1 \ln \left( \frac{R_y}{R_1} \right) \text{sgn}(\tau_i) \\ &= \Omega + \frac{B R_1}{2} \left( \frac{|\tau_i|}{B} \left( \frac{R_1^2}{R_y^2} - 1 \right) + \ln \left( \frac{R_y}{R_1} \right)^2 \right) \text{sgn}(\tau_i) \\ &= \Omega + \frac{B R_1}{2} \left( \frac{|\tau_i|}{B} \left( \frac{B}{|\tau_i|} - 1 \right) + \ln \left( \frac{|\tau_i|}{B} \right) \right) \text{sgn}(\tau_i) \end{aligned} \quad (2.36)$$

or

$$\Omega - 1 = -\frac{B R_1}{2} \left( \ln \left( \frac{|\tau_i|}{B} \right) - \frac{|\tau_i|}{B} + 1 \right) \text{sgn}(\tau_i). \quad (2.37)$$

If we are in region II, then  $1 < \frac{|\tau_i|}{B} \leq \frac{1}{\eta^2}$ , therefore  $\ln \left( \frac{|\tau_i|}{B} \right) - \frac{|\tau_i|}{B} + 1 < 0$ . Again we obtain  $\tau_i < 0 \Leftrightarrow \Omega < 1$  and  $\tau_i > 0 \Leftrightarrow \Omega > 1$ . Therefore,

$$\text{sgn}(\tau_i) = \text{sgn}(\Omega - 1). \quad (2.38)$$

Let

$$F(\tau_i) = V(R_1) - 1 = \Omega - 1 + H(\tau_i) \text{sgn}(\tau_i) \quad (2.39)$$

where

$$H(\tau_i) = \frac{B R_1}{2} \left( \ln \left( \frac{|\tau_i|}{B} \right) - \frac{|\tau_i|}{B} + 1 \right). \quad (2.40)$$

We want to find a  $\tau_i$  such that  $F(\tau_i) = 0$  with  $B < |\tau_i| \leq B/\eta^2$ . Note that for  $\tau_i > 0$

$$F'(\tau_i) = \frac{BR_1}{2} \left( \frac{1}{\tau_i} - \frac{1}{B} \right) < 0 \quad (2.41)$$

so that  $F$  is strictly decreasing on  $(B, \infty)$  with  $F(B) = \Omega - 1 > 0$ . This result implies that we can solve for  $\tau_i$  numerically for example by using a bisection method on  $F$ . Furthermore,  $F(\tau_i)$  is an odd function so that if  $\tau_i < 0$ ,  $F'(\tau_i)$  is strictly decreasing on  $(-\infty, -B)$  with  $F(-B) = \Omega - 1 < 0$  so that we can also use the bisection method for  $\tau_i < -B$  (see section 4.2.1).

## 2.5 Visualizing Regions I, II and III

In this section, we would like to determine how to represent regions I, II and III on the  $(Re_2, Re_2)$ -plane. Let us first begin by noting that we can express  $Re_1$  in terms of  $Re_2$  as

$$Re_1 = \frac{\eta}{\Omega} Re_2. \quad (2.42)$$

Note that if we are in region III, then  $\Omega = 1$  or

$$Re_1 = \eta Re_2. \quad (2.43)$$

If we are in region I with  $\frac{\tau_i}{B} > \frac{1}{\eta^2} > 0$ , then we obtain the relation

$$\Omega - 1 = -\frac{BR_1}{2} \left( \frac{\tau_i}{B} (\eta^2 - 1) + \ln \left( \frac{1}{\eta^2} \right) \right) > G \quad (2.44)$$

where

$$G = -\frac{BR_1}{2} \left( \ln \left( \frac{1}{\eta^2} \right) - \frac{1}{\eta^2} + 1 \right) > 0. \quad (2.45)$$

Since  $\Omega > 1 + G > 0$ , equation (2.44) can be rearranged to read  $1/\Omega < 1/(1 + G)$ . Therefore, there is no plug if

$$Re_1 < \frac{\eta}{1+G} Re_2. \quad (2.46)$$

Consider the other no plug case where  $\frac{\tau_i}{B} < -\frac{1}{\eta^2} < 0$ . Equation (2.33) gives

$$1 - \Omega = -\frac{BR_1}{2} \left( \frac{|\tau_i|}{B} (\eta^2 - 1) + \ln \left( \frac{1}{\eta^2} \right) \right) > G \quad (2.47)$$

which can be arranged to read  $\Omega < 1 - G < 1$ . It follows that

$$Re_2 = \frac{\Omega}{\eta} Re_1 < \frac{1-G}{\eta} Re_1 \quad (2.48)$$

The no plug region with  $\tau_i < -B/\eta^2$  will fall into one of the three cases below:

$$1 - G > 0 : Re_1 > \frac{\eta}{1-G} Re_2 \quad (2.49)$$

$$1 - G < 0 : Re_1 < \frac{\eta}{1-G} Re_2 \quad (2.50)$$

$$1 - G = 0 : Re_2 < 0. \quad (2.51)$$

Figure 2.1 shows where the regions fall on the  $(Re_2, Re_1)$ -plane for different values of  $B$  with  $\eta = 0.883$ . It is clear that as the Bingham number increases, region II increases. Note that region III is a line. It is the rigid rotation line  $Re_1 = \eta Re_2$  and it stays the same for all  $B$ . For a fixed value of  $B$ , figure 2.2 shows that region II decreases as  $\eta$  increases.

## 2.6 Limit as $B \rightarrow 0$

In this section, our goal is to show continuity of the flow with respect to  $B$ . As  $B \rightarrow 0$ ,  $R_y \rightarrow \infty$  so that  $R_o = R_2$  which implies that we need to take the limit of the velocity profile in region I. Rewrite the velocity profile as

$$V(r) = A_1 r + \frac{A_2}{r} - Br \ln(r) \text{sgn}(\tau_i) \quad (2.52)$$

Chapter 2. Governing Equations

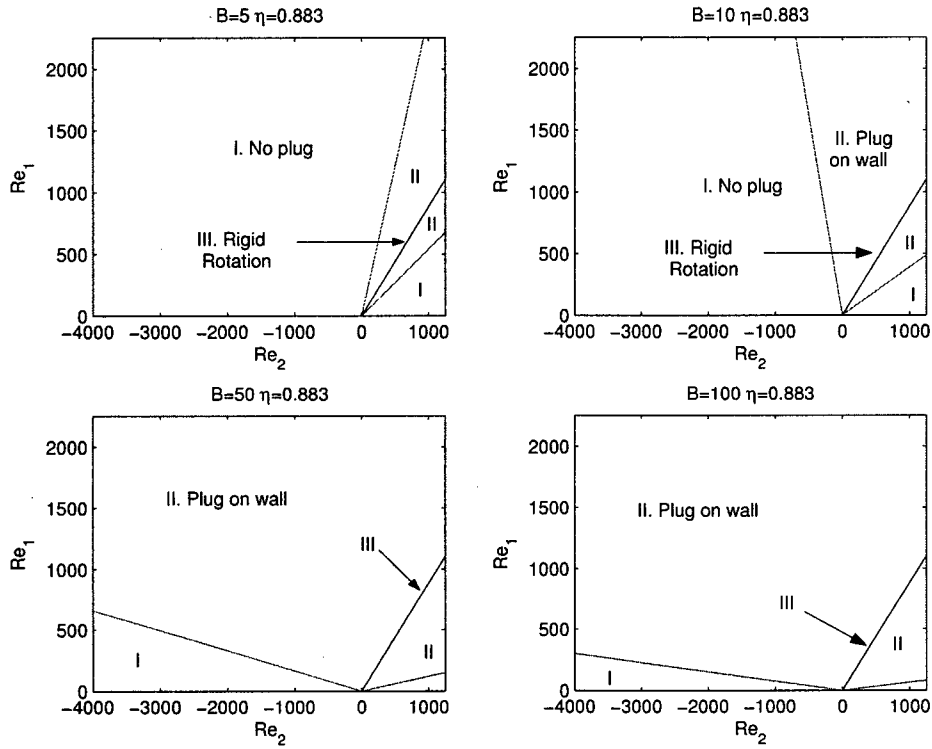


Figure 2.1: Regions with  $\eta = 0.883$  for various values of  $B$ . Region III is the line  $Re_1 = \eta Re_2$ .

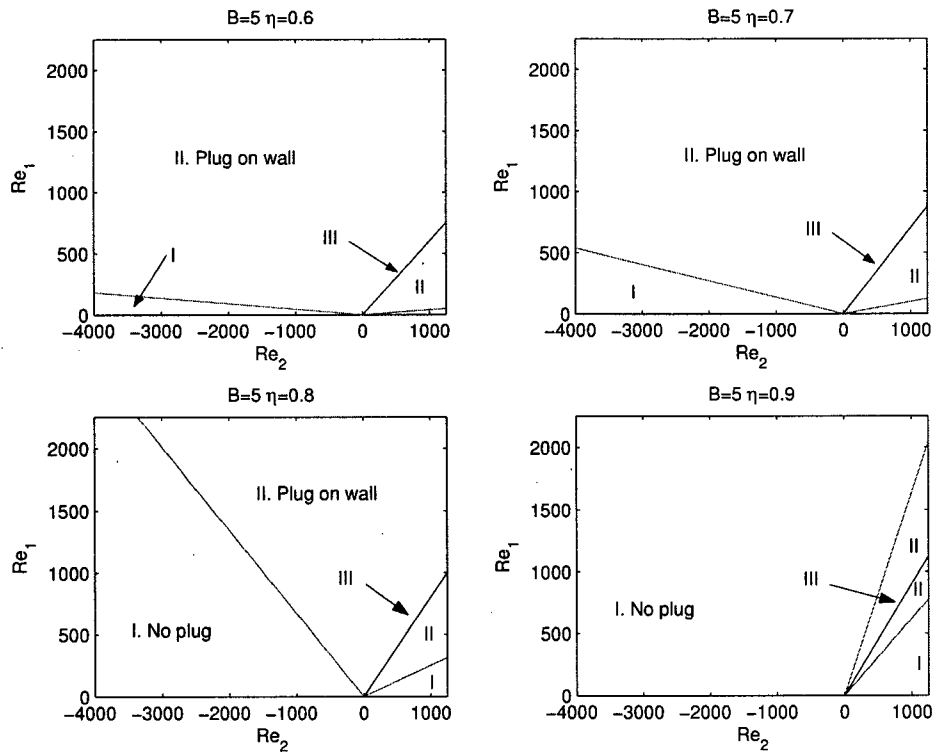


Figure 2.2: Regions with  $B = 5$  for various values of  $\eta$ .

where

$$A_1 = \frac{\Omega}{R_1} + \frac{\tau_i R_1^2}{2R_2^2} + B \ln R_2 \operatorname{sgn}(\tau_i) \quad (2.53)$$

and

$$A_2 = -\frac{1}{2}\tau_i R_1^2. \quad (2.54)$$

First, let us determine the relationship between  $\Omega$  and  $\tau_i$  as  $B \rightarrow 0$ . From equation (2.32) it follows that

$$1 - \Omega = \lim_{B \rightarrow 0} \left\{ \frac{1}{2}\tau_i R_1 (\eta^2 - 1) + B R_1 \ln \left( \frac{1}{\eta} \right) \operatorname{sgn}(\tau_i) \right\} = \frac{\tau_i}{2} \left( \frac{\eta}{1 - \eta} \right) (\eta^2 - 1). \quad (2.55)$$

Therefore as  $B \rightarrow 0$ , we obtain

$$\frac{\tau_i}{2} = \left( \frac{1 - \eta}{\eta} \right) \left( \frac{1 - \Omega}{\eta^2 - 1} \right). \quad (2.56)$$

Taking the limits as  $B \rightarrow 0$  of  $A_1$  and  $A_2$  and using equation (2.56) gives

$$\lim_{B \rightarrow 0} A_1 = \Omega \left( \frac{1 - \eta}{\eta} \right) + \left( \frac{1 - \eta}{\eta} \right) \left( \frac{1 - \Omega}{\eta^2 - 1} \right) \left( \frac{R_1}{R_2} \right)^2 = \frac{(1 - \eta)(\Omega - \eta^2)}{\eta(1 - \eta^2)} \quad (2.57)$$

$$\lim_{B \rightarrow 0} A_2 = \left( \frac{1 - \Omega}{1 - \eta^2} \right) \left( \frac{\eta}{1 - \eta} \right) \quad (2.58)$$

so that as  $B \rightarrow 0$  we obtain the velocity profile

$$V(r) = \frac{(1 - \eta)(\Omega - \eta^2)}{\eta(1 - \eta^2)} r + \left( \frac{1 - \Omega}{1 - \eta^2} \right) \left( \frac{\eta}{1 - \eta} \right) \frac{1}{r} \quad (2.59)$$

for  $\frac{\eta}{1 - \eta} \leq r \leq \frac{1}{1 - \eta}$  which is that of a Newtonian fluid in Couette flow [10].

# Chapter 3

## Linear Stability Analysis

To determine for what values of  $Re_1$  and  $Re_2$  the primary instability occurs, we will follow the method in [6] by adding a small perturbation to the basic flow, and determining whether this perturbation grows or decays with time. By assuming a normal mode solution for this perturbation, the linearized perturbation equations become a system of ordinary rather than partial differential equations, which leads to an eigenvalue problem. Furthermore, boundary conditions for the perturbation will be derived. In addition to the no slip boundary conditions on the cylinder walls, a boundary condition needs to be applied to the plug region in the case of type II flow.

### 3.1 Linear Perturbation Equations

For now, consider some arbitrary basic, steady flow  $(\mathbf{U}, P)$  where  $\mathbf{U}$  is the basic velocity and  $P$  the basic pressure. We would like to examine the linear stability of  $\mathbf{U}$  by introducing a small disturbance in the velocity of the form

$$\epsilon \mathbf{u}' = (\epsilon u'(r, \theta, z, t), \epsilon v'(r, \theta, z, t), w'(r, \theta, z, t)) \quad (3.1)$$

and in the pressure

$$\epsilon p'(r, \theta, z, t) \quad (3.2)$$

where  $\epsilon \ll 1$ . The perturbed flow is expressed as  $\mathbf{U} + \epsilon \mathbf{u}'$ ,  $P + \epsilon p'$ . Both the basic flow and the perturbed flow satisfy the Navier-Stokes and the continuity equation. That is, the perturbed

flow satisfies

$$\nabla \cdot (\mathbf{U} + \epsilon \mathbf{u}') = 0 \quad (3.3)$$

$$\epsilon \mathbf{u}'_t + Re_1(\mathbf{U} + \epsilon \mathbf{u}') \cdot \nabla(\mathbf{U} + \epsilon \mathbf{u}') = -\nabla(P + \epsilon p') + \nabla \cdot \tau(\mathbf{U} + \epsilon \mathbf{u}') \quad (3.4)$$

and the basic flow satisfies

$$\nabla \cdot \mathbf{U} = 0 \quad (3.5)$$

$$Re_1(\mathbf{U} \cdot \nabla)\mathbf{U} = -\nabla P + \nabla \cdot \tau(\mathbf{U}). \quad (3.6)$$

Subtracting equation (3.5) from (3.3) gives the perturbed continuity equation

$$\nabla \cdot \mathbf{u}' = \frac{\partial u'}{\partial r} + \frac{u'}{r} + \frac{1}{r} \frac{\partial v'}{\partial \theta} + \frac{\partial w'}{\partial z} = 0. \quad (3.7)$$

Subtracting equation (3.6) from (3.4) gives

$$\epsilon(\mathbf{u}'_t + Re_1(\mathbf{u}' \cdot \nabla)\mathbf{U} + (\mathbf{U} \cdot \nabla)\mathbf{u}') + \epsilon^2 Re_1(\mathbf{u}' \cdot \nabla)\mathbf{u}' = -\epsilon \nabla p + \nabla \cdot (\tau(\mathbf{U} + \epsilon \mathbf{u}') - \tau(\mathbf{U})). \quad (3.8)$$

Note that  $\tau$  is determined only in regions where  $\tau > B$ . Suppose we are in a region where both  $\tau(\mathbf{U} + \epsilon \mathbf{u}') > B$  and  $\tau(\mathbf{U}) > B$ . Then we have,

$$\tau_{ij}(\mathbf{U} + \epsilon \mathbf{u}') - \tau_{ij}(\mathbf{U}) = \mu_e(\mathbf{U} + \epsilon \mathbf{u}') \dot{\gamma}_{ij}(\mathbf{U} + \epsilon \mathbf{u}') - \mu_e(\mathbf{U}) \dot{\gamma}_{ij}(\mathbf{U}) \quad (3.9)$$

where

$$\mu_e = 1 + \frac{B}{\dot{\gamma}}. \quad (3.10)$$

Using the fact that  $\dot{\gamma}_{ij}(\mathbf{U} + \epsilon \mathbf{u}') = \dot{\gamma}_{ij}(\mathbf{U}) + \epsilon \dot{\gamma}_{ij}(\mathbf{u}')$ , we linearize  $\mu_e(\mathbf{U} + \epsilon \mathbf{u}')$  about the basic flow  $\mathbf{U}$  to obtain

$$\mu_e(\mathbf{U} + \epsilon \mathbf{u}') = \mu_e(\mathbf{U}) + \epsilon \sum_{mn} \dot{\gamma}_{mn}(\mathbf{u}') \frac{\partial \mu_e(\mathbf{U})}{\partial \dot{\gamma}_{mn}} + O(\epsilon^2). \quad (3.11)$$

Note that

$$\frac{\partial \mu_e}{\partial \dot{\gamma}_{mn}} = \frac{\partial \mu_e}{\partial \dot{\gamma}} \frac{\partial \dot{\gamma}}{\partial \dot{\gamma}_{mn}} = \frac{\partial \mu_e}{\partial \dot{\gamma}} \left( \frac{1}{2} \frac{\dot{\gamma}_{mn}}{\dot{\gamma}} \right) = \frac{1}{2} \frac{\partial}{\partial \dot{\gamma}} (1 + B \dot{\gamma}^{-1}) \frac{\dot{\gamma}_{mn}}{\dot{\gamma}} = -\frac{1}{2} B \dot{\gamma}_{mn} \dot{\gamma}^{-3}. \quad (3.12)$$

Substituting this result into equation (3.11) gives

$$\begin{aligned} \mu_e(\mathbf{U} + \epsilon \mathbf{u}') &= \mu_e(\mathbf{U}) - \epsilon \frac{B}{2 \dot{\gamma}(\mathbf{U})^3} \sum_{mn} \dot{\gamma}_{mn}(\mathbf{u}') \dot{\gamma}_{mn}(\mathbf{U}) + O(\epsilon^2) \\ &= \mu_e(\mathbf{U}) - \epsilon \frac{B}{\dot{\gamma}(\mathbf{U})^3} \dot{\gamma}_{r\theta}(\mathbf{u}') \dot{\gamma}_{r\theta}(\mathbf{U}) + O(\epsilon^2). \end{aligned} \quad (3.13)$$

Substitute this result into equation (3.9) to obtain

$$\begin{aligned}
 & \tau_{ij}(\mathbf{U} + \epsilon \mathbf{u}') - \tau_{ij}(\mathbf{U}) \\
 = & \left( \mu_e(\mathbf{U}) - \epsilon \frac{B}{\gamma^3} \dot{\gamma}_{r\theta}(\mathbf{u}') \dot{\gamma}_{r\theta}(\mathbf{U}) \right) (\dot{\gamma}_{ij}(\mathbf{U}) + \epsilon \dot{\gamma}_{ij}(\mathbf{u}')) - \mu_e(\mathbf{U}) \dot{\gamma}_{ij}(\mathbf{U}) + O(\epsilon^2) \\
 = & \epsilon \left( \mu_e(\mathbf{U}) \dot{\gamma}_{ij}(\mathbf{u}') - \frac{B}{\gamma^3} \dot{\gamma}_{ij}(\mathbf{U}) \dot{\gamma}_{r\theta}(\mathbf{U}) \dot{\gamma}_{r\theta}(\mathbf{u}') \right) + O(\epsilon^2) \\
 = & \epsilon \begin{cases} \mu_e(\mathbf{U}) \dot{\gamma}_{ij}(\mathbf{u}'), & ij \neq r\theta, \theta r \\ \mu_e(\mathbf{U}) \dot{\gamma}_{ij}(\mathbf{u}') - B \frac{\dot{\gamma}_{ij}(\mathbf{u}')}{\dot{\gamma}(\mathbf{U})}, & ij = r\theta, \theta r \end{cases} + O(\epsilon^2) \\
 = & \epsilon \begin{cases} \mu_e(\mathbf{U}) \dot{\gamma}_{ij}(\mathbf{u}'), & ij \neq r\theta, \theta r \\ \dot{\gamma}_{ij}(\mathbf{u}') & ij = r\theta, \theta r \end{cases} + O(\epsilon^2) \\
 = & \epsilon \begin{cases} \dot{\gamma}_{ij}(\mathbf{u}') + B \frac{\dot{\gamma}_{ij}(\mathbf{u}')}{\dot{\gamma}(\mathbf{U})}, & ij \neq r\theta, \theta r \\ \dot{\gamma}_{ij}(\mathbf{u}') & ij = r\theta, \theta r \end{cases} + O(\epsilon^2) \\
 = & \epsilon \begin{cases} \dot{\gamma}_{ij}(\mathbf{u}') + B M_{ij} & ij \neq r\theta, \theta r \\ \dot{\gamma}_{ij}(\mathbf{u}') & ij = r\theta, \theta r \end{cases} + O(\epsilon^2) \tag{3.14}
 \end{aligned}$$

where  $M_{ij} = \frac{\dot{\gamma}_{ij}(\mathbf{u}')}{\dot{\gamma}(\mathbf{U})}$ . After some algebra, we find that

$$\mathbf{u}' \cdot \nabla \mathbf{U} + \mathbf{U} \cdot \nabla \mathbf{u}' = \frac{V}{r} \left( \frac{\partial u'}{\partial \theta} - 2v' \right) \mathbf{e}_r + \left( u' \frac{dV}{dr} + u' \frac{V}{r} + \frac{V}{r} \frac{\partial v'}{\partial \theta} \right) \mathbf{e}_\theta + \left( \frac{V}{r} \frac{\partial w'}{\partial \theta} \right) \mathbf{e}_z.$$

Substituting this result, and our expression for  $\tau_{ij}(\mathbf{U} + \epsilon \mathbf{u}') - \tau_{ij}(\mathbf{U})$  into equation (3.8), and retaining terms of order  $\epsilon$  gives

$$\begin{aligned}
 \frac{\partial u'}{\partial t} + Re_1 \frac{V}{r} \left( \frac{\partial u'}{\partial \theta} - 2v' \right) &= -\frac{\partial p'}{\partial r} + \frac{1}{r} \frac{\partial}{\partial r} (r \dot{\gamma}_{rr}(\mathbf{u}')) + \frac{1}{r} \frac{\partial}{\partial \theta} (\dot{\gamma}_{r\theta}(\mathbf{u}')) + \frac{\partial}{\partial z} (\dot{\gamma}_{rz}(\mathbf{u}')) - \frac{1}{r} \dot{\gamma}_{\theta\theta} \\
 &+ B \left( \frac{1}{r} \frac{\partial}{\partial r} (r M_{rr}) + \frac{\partial}{\partial z} (M_{rz}) - \frac{1}{r} M_{r\theta} \right) \tag{3.15}
 \end{aligned}$$

$$\begin{aligned} \frac{\partial v'}{\partial t} + Re_1 \left( u' \frac{dV}{dr} + u' \frac{V}{r} + \frac{V}{r} \frac{\partial v'}{\partial \theta} \right) &= -\frac{1}{r} \frac{\partial p'}{\partial \theta} + \frac{1}{r^2} \frac{\partial}{\partial r} (r^2 \dot{\gamma}_{r\theta}) + \frac{1}{r} \frac{\partial}{\partial \theta} (\dot{\gamma}_{\theta\theta}) + \frac{\partial}{\partial z} (\dot{\gamma}_{\theta z}) \\ &+ B \left( \frac{1}{r} \frac{\partial}{\partial \theta} (M_{\theta\theta}) + \frac{\partial}{\partial z} (M_{\theta z}) \right) \end{aligned} \quad (3.16)$$

$$\begin{aligned} \frac{\partial w'}{\partial t} + Re_1 \left( \frac{V}{r} \frac{\partial w'}{\partial \theta} \right) &= -\frac{\partial p'}{\partial z} + \frac{1}{r} \frac{\partial}{\partial r} (r \dot{\gamma}_{zr}) + \frac{1}{r} \frac{\partial}{\partial \theta} (\dot{\gamma}_{z\theta}) + \frac{\partial}{\partial z} (\dot{\gamma}_{zz}) \\ &+ B \left( \frac{1}{r} \frac{\partial}{\partial r} (r M_{zr}) + \frac{1}{r} \frac{\partial}{\partial \theta} (M_{z\theta}) + \frac{\partial}{\partial z} (M_{zz}) \right). \end{aligned} \quad (3.17)$$

Simplifying the above equations gives the following linearized perturbation equations

$$\begin{aligned} \frac{\partial u'}{\partial t} + Re_1 \frac{V}{r} \left( \frac{\partial u'}{\partial \theta} - 2v' \right) &= -\frac{\partial p'}{\partial r} + \nabla^2 u' - \frac{2}{r^2} \frac{\partial v'}{\partial \theta} - \frac{u'}{r^2} \\ &+ B \left\{ \frac{1}{r} \frac{\partial}{\partial r} \left( \frac{r \dot{\gamma}_{rr}(\mathbf{u}')}{\dot{\gamma}(\mathbf{U})} \right) + \frac{1}{\dot{\gamma}} \left( \frac{\partial \dot{\gamma}_{rz}(\mathbf{u}')}{\partial z} - \frac{\dot{\gamma}_{\theta\theta}(\mathbf{u}')}{r} \right) \right\} \end{aligned} \quad (3.18)$$

$$\begin{aligned} \frac{\partial v'}{\partial t} + Re_1 \left( u' D_* V + \frac{V}{r} \frac{\partial v'}{\partial \theta} \right) &= -\frac{1}{r} \frac{\partial p'}{\partial \theta} + \nabla^2 v' + \frac{2}{r^2} \frac{\partial u'}{\partial \theta} - \frac{v'}{r^2} \\ &+ B \frac{1}{\dot{\gamma}} \left\{ \frac{1}{r} \frac{\partial \dot{\gamma}_{\theta\theta}(\mathbf{u}')}{\partial \theta} + \frac{\partial \dot{\gamma}_{\theta z}(\mathbf{u}')}{\partial z} \right\} \end{aligned} \quad (3.19)$$

$$\begin{aligned} \frac{\partial w'}{\partial t} + Re_1 \frac{V}{r} \frac{\partial w'}{\partial \theta} &= -\frac{\partial p'}{\partial z} + \nabla^2 w' \\ &+ B \left\{ \frac{1}{r} \frac{\partial}{\partial r} \left( r \frac{\dot{\gamma}_{zr}(\mathbf{u}')}{\dot{\gamma}} \right) + \frac{1}{\dot{\gamma}} \left( \frac{1}{r} \frac{\partial \dot{\gamma}_{z\theta}(\mathbf{u}')}{\partial \theta} + \frac{\partial \dot{\gamma}_{zz}(\mathbf{u}')}{\partial z} \right) \right\} \end{aligned} \quad (3.20)$$

where  $D_* = \frac{d}{dr} + \frac{1}{r}$  and  $\dot{\gamma} = \dot{\gamma}(\mathbf{U})$  where

$$\dot{\gamma} = |\dot{\gamma}_{r\theta}| = \frac{|\tau_i| R_1^2}{r^2} - B \quad (3.21)$$

As required,  $\dot{\gamma}$  is nonnegative on  $[R_1, R_o]$  since it is decreasing on that interval with  $\dot{\gamma}(R_1) = |\tau_i| - B > 0$  and  $\dot{\gamma}(R_y) = 0$  or  $\dot{\gamma}(R_2) > 0$ . Note that if we are in region II, there is a singularity in equations (3.18)-(3.20) since in the denominator we will have  $\dot{\gamma}(R_y) = 0$ . This singularity, however, is remedied by the boundary conditions (3.60) that we will derive in section 3.3. These boundary conditions help to define the linear perturbation equations as  $r \rightarrow R_y$ .

### 3.2 The Method of Normal Modes

This system of PDEs can be reduced to a system of ODEs by applying the method of normal modes. That is, by assuming a solution of the form

$$(u', v', w', p') = e^{\lambda t + i(m\theta + kz)}(u(r), v(r), w(r), p(r)). \quad (3.22)$$

Let  $D = \frac{d}{dr}$  and substitute the above into each strain rate component  $\dot{\gamma}_{ij}$  to obtain

$$\dot{\gamma}_{rr}(\mathbf{u}') = 2 \frac{\partial u'}{\partial r} = 2Du e^{\lambda t + i(m\theta + kz)} \quad (3.23)$$

$$\dot{\gamma}_{r\theta}(\mathbf{u}') = \frac{1}{r} \left( \frac{\partial u'}{\partial \theta} - v' \right) + \frac{\partial v'}{\partial r} = \left( \frac{1}{r} (imu - v) + Dv \right) e^{\lambda t + i(m\theta + kz)} \quad (3.24)$$

$$\dot{\gamma}_{rz}(\mathbf{u}') = \frac{\partial u'}{\partial z} + \frac{\partial w'}{\partial r} = (iku + Dw) e^{\lambda t + i(m\theta + kz)} \quad (3.25)$$

$$\dot{\gamma}_{\theta\theta}(\mathbf{u}') = \frac{2}{r} \left( \frac{\partial v'}{\partial \theta} + u' \right) = \frac{2}{r} (imv + u) e^{\lambda t + i(m\theta + kz)} \quad (3.26)$$

$$\dot{\gamma}_{\theta z}(\mathbf{u}') = \frac{1}{r} \frac{\partial w'}{\partial \theta} + \frac{\partial v'}{\partial z} = \left( \frac{1}{r} imw + kv \right) e^{\lambda t + i(m\theta + kz)} \quad (3.27)$$

$$\dot{\gamma}_{zz}(\mathbf{u}') = 2 \frac{\partial w'}{\partial z} = 2ikw e^{\lambda t + i(m\theta + kz)}. \quad (3.28)$$

Let

$$\alpha = \lambda t + i(m\theta + kz) \quad (3.29)$$

and substitute all of the above into the Bingham terms of the linearized perturbation equations (3.18) - (3.20). The Bingham terms in equation (3.18) become

$$\begin{aligned} & \frac{1}{r} \frac{\partial}{\partial r} \left( r \frac{\dot{\gamma}_{rr}(\mathbf{u}')}{\dot{\gamma}} \right) + \frac{1}{\dot{\gamma}} \left( \frac{\partial \dot{\gamma}_{rz}(\mathbf{u}')}{\partial z} - \frac{\dot{\gamma}_{\theta\theta}(\mathbf{u}')}{r} \right) \\ = & \frac{1}{r} \frac{\partial}{\partial r} \left( \frac{2rDue^\alpha}{\dot{\gamma}} \right) + \frac{1}{\dot{\gamma}} \frac{\partial}{\partial z} ((iku + Dw)e^\alpha) - \frac{2}{r^2 \dot{\gamma}} (imv + u) e^\alpha \\ = & \left( \frac{1}{r} \frac{\partial}{\partial r} \left( \frac{2rDu}{\dot{\gamma}} \right) + \frac{-k^2u + ikDw}{\dot{\gamma}} - \frac{2}{r^2 \dot{\gamma}} (imv + u) \right) e^\alpha \end{aligned} \quad (3.30)$$

while for equation (3.19) the Bingham terms can be expressed as

$$\begin{aligned} & \frac{1}{\dot{\gamma}} \left( \frac{1}{r} \frac{\partial \dot{\gamma}_{\theta\theta}(\mathbf{u}')}{\partial \theta} + \frac{\partial \dot{\gamma}_{\theta z}(\mathbf{u}')}{\partial z} \right) \\ = & \frac{1}{r\dot{\gamma}} \frac{\partial}{\partial \theta} \left( \frac{2}{r} (imv + u) e^\alpha \right) + \frac{1}{\dot{\gamma}} \frac{\partial}{\partial z} \left( \left( \frac{1}{r} imw + ikv \right) e^\alpha \right) \\ = & \frac{1}{\dot{\gamma}} \left( \frac{2}{r^2} (imu - m^2v) - \frac{mkw}{r} - k^2v \right) e^\alpha \end{aligned} \quad (3.31)$$

and for equation (3.20) they can be rewritten as

$$\begin{aligned} & \frac{1}{r} \frac{\partial}{\partial r} \left( r \frac{\dot{\gamma}_{zr}(\mathbf{u}')}{\dot{\gamma}} \right) + \frac{1}{\dot{\gamma}} \left( \frac{1}{r} \frac{\partial \dot{\gamma}_{z\theta}(\mathbf{u}')}{\partial \theta} + \frac{\partial \dot{\gamma}_{zz}(\mathbf{u}')}{\partial z} \right) \\ = & \frac{1}{r} \frac{\partial}{\partial r} \left( \frac{r(iku + Dw)}{\dot{\gamma}} e^\alpha \right) + \frac{1}{r\dot{\gamma}} \frac{\partial}{\partial \theta} \left( \left( \frac{imw}{r} + ikv \right) e^\alpha \right) + \frac{1}{\dot{\gamma}} \frac{\partial}{\partial z} (2ikwe^\alpha) \\ = & \left( \frac{1}{r} \frac{\partial}{\partial r} \left( \frac{r(iku + Dw)}{\dot{\gamma}} \right) + \frac{1}{r\dot{\gamma}} \left( \frac{-m^2w}{r} - kmv \right) + \frac{1}{\dot{\gamma}} (-2k^2w) \right) e^\alpha \\ = & \left( \frac{1}{r} \frac{\partial}{\partial r} \left( \frac{r(iku + Dw)}{\dot{\gamma}} \right) - \frac{1}{\dot{\gamma}} \left( \frac{m^2w}{r^2} + \frac{kmv}{r} + 2k^2w \right) \right) e^\alpha. \end{aligned} \quad (3.32)$$

Define

$$\phi_r(r, u, v, w, Du, Dv, Dw) = \frac{1}{r}D \left( \frac{2rDu}{\dot{\gamma}} \right) + \frac{1}{\dot{\gamma}} \left( ikDw - k^2u - \frac{2(imv + u)}{r^2} \right) \quad (3.33)$$

$$\phi_\theta(r, u, v, w, Du, Dv, Dw) = \frac{1}{\dot{\gamma}} \left( \frac{2(imu - m^2v)}{r^2} - \frac{kmw}{r} - k^2v \right) \quad (3.34)$$

$$\phi_z(r, u, v, w, Du, Dv, Dw) = \frac{1}{r}D \left( \frac{r(iku + Dw)}{\dot{\gamma}} \right) - \frac{1}{\dot{\gamma}} \left( \frac{m^2w}{r^2} + \frac{kmv}{r} + 2k^2w \right). \quad (3.35)$$

Then, substituting expressions (3.22) and (3.33)-(3.35) into the linearized perturbation equations (3.7) and (3.18)-(3.20) gives

$$\lambda u + Re_1 \frac{V}{r} (imu - 2v) = -Dp + D^2u + \frac{Du}{r} - \frac{m^2u}{r^2} - k^2u - \frac{2imv}{r^2} - \frac{u}{r^2} + B\phi_r \quad (3.36)$$

$$\begin{aligned} \lambda v + Re_1 \left( uD_*V + \frac{V}{r}imv \right) &= -\frac{im}{r}p + D^2v + \frac{Dv}{r} - \frac{m^2}{r^2}v - k^2v \\ &+ \frac{2im}{r^2}u - \frac{v}{r^2} + B\phi_\theta \end{aligned} \quad (3.37)$$

$$\lambda w + Re_1 \frac{V}{r} imw = -ikp + D^2w + \frac{Dw}{r} - \frac{m^2}{r^2}w - k^2w + B\phi_z \quad (3.38)$$

$$D_*u + \frac{mv}{r} + ikw = 0. \quad (3.39)$$

### 3.3 Boundary Conditions for the Perturbation

The boundary conditions for the perturbation are divided into two cases: no plug and plug on the wall.

#### 3.3.1 Region I: No Plug

From the no-slip conditions at the cylinder walls, it follows that

$$u = v = w = 0 \text{ at } r = R_1, r = R_2. \quad (3.40)$$

Equation (3.39) implies that we can rewrite the boundary conditions as

$$u = Du = v = 0 \text{ at } r = R_1, r = R_2. \quad (3.41)$$

### 3.3.2 Region II: Plug on the Wall

In addition to the zero boundary conditions at  $r = R_1$  and  $r = R_2$ , we must apply boundary conditions at the yield surface  $r = R_y$ . Since the velocity and pressure are being perturbed, then the stress is being perturbed, so the yield surface must also be perturbed. Since the perturbations are periodic, we assume that the yield surface has also been perturbed in a periodic manner, so we write the perturbed yield surface as

$$r = R_y + \epsilon h(\theta, z, t) \quad (3.42)$$

where  $h = h_o e^{\lambda t + i(m\theta + kz)}$  and  $h_o$  is a constant. The yield criterion along with continuity of stress suggests that  $\dot{\gamma}(\mathbf{U} + \epsilon \mathbf{u}') = 0$  at the perturbed yield surface. That is,

$$\dot{\gamma}_{ij}(\mathbf{U} + \epsilon \mathbf{u}') = 0, \quad r = R_y + \epsilon h, \quad i, j = r, \theta, z. \quad (3.43)$$

Let

$$\dot{\Gamma}_{ij} = \dot{\gamma}_{ij}(\mathbf{U}(R_y + \epsilon h) + \epsilon \mathbf{u}'(R_y + \epsilon h, \theta, z, t)). \quad (3.44)$$

Evaluating the perturbed strain rate at the perturbed yield surface, and linearizing about  $r = R_y$ , it follows from equations (3.23)-(3.28) that

$$\dot{\Gamma}_{rr} = 2\epsilon Du(R_y + \epsilon h)e^\alpha = 2\epsilon Du(R_y)e^\alpha + O(\epsilon^2) \quad (3.45)$$

$$\dot{\Gamma}_{rz} = \epsilon (iku(R_y + \epsilon h) + Dw(R_y + \epsilon h)) e^\alpha = \epsilon (iku(R_y) + Dw(R_y)) e^\alpha + O(\epsilon^2) \quad (3.46)$$

$$\dot{\Gamma}_{\theta\theta} = 2\epsilon \left( im \frac{v(R_y + \epsilon h)}{R_y + \epsilon h} + \frac{u(R_y + \epsilon h)}{R_y + \epsilon h} \right) e^\alpha = 2\epsilon \left( im \frac{v(R_y)}{R_y} + \frac{u(R_y)}{R_y} \right) e^\alpha + O(\epsilon^2) \quad (3.47)$$

$$\dot{\Gamma}_{\theta z} = \epsilon \left( im \frac{w(R_y + \epsilon h)}{R_y + \epsilon h} + ikv(R_y + \epsilon h) \right) e^\alpha = \epsilon \left( im \frac{w(R_y)}{R_y} + ikv(R_y) \right) e^\alpha + O(\epsilon^2) \quad (3.48)$$

$$\dot{\Gamma}_{zz} = 2\epsilon ikw(R_y + \epsilon h) e^\alpha = 2\epsilon ikw(R_y) e^\alpha + O(\epsilon^2) \quad (3.49)$$

$$\dot{\Gamma}_{r\theta} = \epsilon \left( im \frac{u(R_y)}{R_y} + Dv(R_y) - \frac{v(R_y)}{R_y} + h_o D^2 V(R_y) \right) e^\alpha + O(\epsilon^2). \quad (3.50)$$

Note that in equation (3.50) we used the fact that  $\dot{\gamma}(R_y) = DV(R_y) - \frac{V(R_y)}{R_y} = 0$ . Using equation (3.43) we will set each  $\Gamma_{ij} = 0$ . Assuming  $k \neq 0$  and retaining terms of order  $\epsilon$  gives

$$0 = Du(R_y^-) \quad (3.51)$$

$$0 = ikw(R_y^-) \quad (3.52)$$

$$0 = imw(R_y^-) + ikR_y v(R_y^-) = ikR_y v(R_y^-) \quad (3.53)$$

$$0 = imv(R_y^-) + u(R_y^-) = u(R_y^-) \quad (3.54)$$

$$0 = iku(R_y^-) + Dw(R_y^-) = Dw(R_y^-) \quad (3.55)$$

$$0 = im \frac{u(R_y^-)}{R_y} + Dv(R_y^-) - \frac{v(R_y^-)}{R_y} + h_o D^2 V(R_y) = Dv(R_y^-) + h_o D^2 V(R_y). \quad (3.56)$$

From the above equations we see that  $\mathbf{u}(R_y^-) = 0$ . We will show that  $\mathbf{u}(R_y) = 0$ . By continuity of velocity, we must have  $\mathbf{U}(R_y^-) + \epsilon \mathbf{u}'(R_y^-, \theta, z, t) = \mathbf{U}(R_y^+) + \epsilon \mathbf{u}'(R_y^+, \theta, z, t)$ . Since the basic

flow  $\mathbf{U}$  is continuous everywhere between the cylinders, we have  $\mathbf{U}(R_y^-) = \mathbf{U}(R_y^+)$ . It follows that  $\mathbf{u}'(R_y^-, \theta, z, t) = \mathbf{u}'(R_y^+, \theta, z, t)$  which implies that  $\mathbf{u}(R_y^-) = \mathbf{u}(R_y^+)$ . Furthermore, we can show that  $\mathbf{u} \equiv 0$  throughout the plug. The boundary conditions at the yield surface are given by

$$u(R_y) = v(R_y) = w(R_y) = 0 \quad (3.57)$$

$$Du(R_y^-) = Dw(R_y^-) = 0, \quad Dv(R_y^-) = -h_o D^2 V(R_y^-).$$

The above boundary conditions together with the fact that

$$D^2 u + \frac{Du}{r} - \frac{u}{r^2} = -im \left( \frac{Dv}{r} - \frac{v}{r^2} \right) - ikDw, \quad (3.58)$$

which follows from the continuity equation, imply the boundary condition

$$D^2 u(R_y^-) = imh_o \frac{D^2 V(R_y^-)}{R_y}. \quad (3.59)$$

Therefore, the boundary conditions in terms of  $u$  and  $v$  are given by

$$u(R_y) = Du(R_y^-) = 0, \quad D^2 u(R_y^-) = imh_o D^2 V(R_y^-) / R_y \quad (3.60)$$

$$v(R_y) = 0, \quad Dv(R_y^-) = -h_o D^2 V(R_y^-).$$

# Chapter 4

## Axisymmetric Disturbance

### 4.1 Axisymmetric Equations

If  $m = 0$ , equations (3.36)-(3.39) become

$$\lambda u - 2Re_1 \left( \frac{V}{r} \right) v = -Dp + D^2u + \frac{Du}{r} - k^2u - \frac{u}{r^2} + B\phi_r \quad (4.1)$$

$$\lambda v + Re_1 u D_* V = D^2v + \frac{Dv}{r} - k^2v - \frac{v}{r^2} - k^2 B \frac{v}{\dot{\gamma}} \quad (4.2)$$

$$\lambda w = -ikp + D^2w + \frac{Dw}{r} - k^2w + B\phi_z \quad (4.3)$$

$$D_* u + ikw = 0 \quad (4.4)$$

where

$$\phi_r(r, u, v, w, Du, Dv, Dw) = \frac{1}{r} D \left( \frac{2rDu}{\dot{\gamma}} \right) + \frac{1}{\dot{\gamma}} \left( ikDw - k^2u - \frac{2u}{r^2} \right) \quad (4.5)$$

$$\phi_z(r, u, v, w, Du, Dv, Dw) = \frac{1}{r} D \left( \frac{r(iku + Dw)}{\dot{\gamma}} \right) - \frac{2k^2w}{\dot{\gamma}}. \quad (4.6)$$

Using the fact that  $DD_* = \frac{d^2}{dr^2} + \frac{1}{r} \frac{d}{dr} - \frac{1}{r^2}$ , and  $D_*D = \frac{d^2}{dr^2} + \frac{1}{r} \frac{d}{dr}$ , we can rewrite equations (4.1) through (4.4) as

$$(DD_* - k^2 - \lambda)u + 2Re_1 \left( \frac{V}{r} \right) v = Dp - B\phi_r \quad (4.7)$$

$$(DD_* - k^2 - \lambda)v = Re_1(D_*V)u + k^2 B \frac{v}{\dot{\gamma}} \quad (4.8)$$

$$(D_*D - k^2 - \lambda)w = ikp - B\phi_z \quad (4.9)$$

$$D_*u = -ikw. \quad (4.10)$$

Substitute equation 4.10 into equation 4.9 to obtain

$$(D_*D - k^2 - \lambda)D_*u = -ik(ikp - B\phi_z) = k^2p + B\Phi_z \quad (4.11)$$

where

$$\begin{aligned} \Phi_z &= ik\phi_z \left( u, v, -\frac{1}{ik}D_*u, Du, Dv, -\frac{1}{ik}DD_*u \right) \\ &= ik \left( \frac{1}{r}D \left( \frac{r(iku + -\frac{1}{ik}DD_*u)}{\dot{\gamma}} \right) - \frac{2k^2(-\frac{1}{ik}D_*u)}{\dot{\gamma}} \right) \\ &= -\frac{1}{r}D \left( \frac{r(k^2u + DD_*u)}{\dot{\gamma}} \right) + \frac{2k^2D_*u}{\dot{\gamma}} \\ &= a_3D^3u + a_2D^2u + a_1Du + a_0u \end{aligned}$$

and the parameters  $a_0$ - $a_3$  are given by

$$a_0 = \frac{k^2}{r\dot{\gamma}} + \frac{k^2 D\dot{\gamma}}{\dot{\gamma}^2} - \frac{D\dot{\gamma}}{r^2\dot{\gamma}^2} - \frac{1}{r^3\dot{\gamma}} \quad (4.12)$$

$$a_1 = \frac{k^2}{\dot{\gamma}} + \frac{1}{r^2\dot{\gamma}} + \frac{D\dot{\gamma}}{r\dot{\gamma}^2} \quad (4.13)$$

$$a_2 = -\frac{2}{r\dot{\gamma}} + \frac{D\dot{\gamma}}{\dot{\gamma}^2} \quad (4.14)$$

$$a_3 = -\frac{1}{\dot{\gamma}}. \quad (4.15)$$

Differentiate equation 4.11 and solve for  $Dp$  to obtain

$$Dp = \frac{1}{k^2} D(D_*D - k^2 - \lambda)D_*u - \frac{1}{k^2} BD\Phi_z. \quad (4.16)$$

Substitute the above expression for  $Dp$  into equation 4.7 to obtain

$$(DD_* - k^2 - \lambda)u + 2Re_1 \frac{V}{r}v = \frac{1}{k^2} D(D_*D - k^2 - \lambda)D_*u - \frac{1}{k^2} BD\Phi_z - B\Phi_r \quad (4.17)$$

where

$$\begin{aligned} \Phi_r &= \phi_r \left( u, v, -\frac{1}{ik} D_*u, Du, Dv, -\frac{1}{ik} DD_*u \right) \\ &= \frac{1}{r} D \left( \frac{2rDu}{\dot{\gamma}} \right) + \frac{1}{\dot{\gamma}} \left( -ik \frac{1}{ik} DD_*u - k^2u - \frac{2u}{r^2} \right) \\ &= \frac{1}{r} D \left( \frac{2rDu}{\dot{\gamma}} \right) - \frac{1}{\dot{\gamma}} \left( DD_*u + k^2u + \frac{2u}{r^2} \right) \\ &= \left( \frac{1}{\dot{\gamma}} \right) D^2u + \left( \frac{1}{r\dot{\gamma}} - \frac{2D\dot{\gamma}}{\dot{\gamma}^2} \right) Du - \left( \frac{1}{r^2\dot{\gamma}} + \frac{k^2}{\dot{\gamma}} \right) u. \end{aligned}$$

Note that

$$\frac{1}{k^2} D(D_*D - k^2 - \lambda)D_*u - (DD_* - k^2 - \lambda)u = \frac{1}{k^2} (DD_* - k^2 - \lambda)(DD_* - k^2)u \quad (4.18)$$

so that we obtain the coupled differential equations

$$(DD_* - k^2 - \lambda)(DD_* - k^2)u = 2k^2 Re_1 \left( \frac{V}{r} \right) v + B (D\Phi_z + k^2\Phi_r) \quad (4.19)$$

$$(DD_* - k^2 - \lambda)v = Re_1(D_*V)u + k^2 B \frac{v}{\dot{\gamma}} \quad (4.20)$$

which can be rewritten as the linear system

$$(M_{Newtonian} + BM_{Bingham}) \begin{pmatrix} u \\ v \end{pmatrix} = \lambda \begin{pmatrix} DD_* - k^2 & 0 \\ 0 & 1 \end{pmatrix} \begin{pmatrix} u \\ v \end{pmatrix} \quad (4.21)$$

where

$$M_{Newtonian} = \begin{pmatrix} (DD_* - k^2)^2 & -2k^2 Re_1 \left( \frac{V}{r} \right) \\ -Re_1(D_*V) & DD_* - k^2 \end{pmatrix} \quad (4.22)$$

and

$$M_{Bingham} = \begin{pmatrix} -\bar{D} & 0 \\ 0 & -\frac{k^2}{\dot{\gamma}} \end{pmatrix}. \quad (4.23)$$

Here,  $\bar{D}$  is the operator which satisfies  $\bar{D}u = D\Phi_z + k^2\Phi_r$ . From equation (4.21) we see that the method of normal modes leads to an eigenvalue problem with eigenvalue  $\lambda$ .

## 4.2 Numerical Methods

In our numerical analysis, given the outer cylinder Reynolds number  $Re_2$ , we would like to determine the inner cylinder Reynolds number  $Re_1$  at which point the primary instability first occurs. If we are in a region where there is a plug on the wall, we will only consider the interval  $[R_1, R_y]$ .

### 4.2.1 Basic Flow Equations

All of the basic flow equations can be fully determined by the set of parameters  $(\eta, B, Re_1, Re_2)$ . Before we calculate any of the flow equations, we first determine the region of interest (I or II) which is dictated by these four parameters as seen in section 2.5. If we are in region I, then  $\tau_i$  is given by equation (2.35). Otherwise, if we are in region II then we apply a bisection method to equation (2.39) searching for a root  $\tau_i$  such that  $F(\tau_i) = 0$ . Since we are in region II, the root  $\tau_i$  must satisfy  $B < |\tau_i| \leq B/\eta^2$ . After having found  $\tau_i$ , we can easily find  $\dot{\gamma}(r; \tau_i, \eta, B)$ ,  $R_o(\tau_i, \eta, B)$  and  $V(r; \tau_i, \eta, B, Re_1, Re_2)$ .

### 4.2.2 Finite Difference Method

Once all the basic properties of the flow have been determined, system (4.21) is fully defined. To approximate the derivatives, we will use a finite difference method over the yielded region  $[R_1, R_o]$  by taking  $N$  data points  $r_1, r_2, \dots, r_N$  where

$$r_i = R_1 + (i - 1) \frac{R_o - R_1}{N - 1}.$$

This mesh leads to an  $(N - 2) \times (N - 2)$  matrix approximation for each derivative (see Appendix A). Hence, system (4.21) becomes a  $(2N - 4) \times (2N - 4)$  eigenvalue problem.

### 4.2.3 Finding the Critical $Re_1$

To find the critical inner cylinder Reynolds number,  $Re_{1_{crit}}$ , we employ a bisection method on  $Re_1$ . Suppose we are working with  $\eta$  and  $B$  fixed. Then for each set of values  $(Re_1, Re_2, k)$  we obtain a spectrum of eigenvalues  $\lambda$ . Let  $\lambda_{max}(k)$  be the eigenvalue with the largest real part for a specific value of  $k$ . Suppose that  $\lambda_{crit}$  is the eigenvalue with the largest real part over all wave numbers  $k$ . That is,  $\text{real}(\lambda_{max}(k)) \leq \text{real}(\lambda_{crit})$  for all  $k$ . Furthermore, suppose that  $\text{real}(\lambda_{max})$  attains its maximum at  $k = k_{crit}$ . Then  $Re_{1_{crit}}$  should satisfy

$$\text{real}(\lambda_{crit}(Re_{1_{crit}}, Re_2, k_{crit})) = 0. \quad (4.24)$$

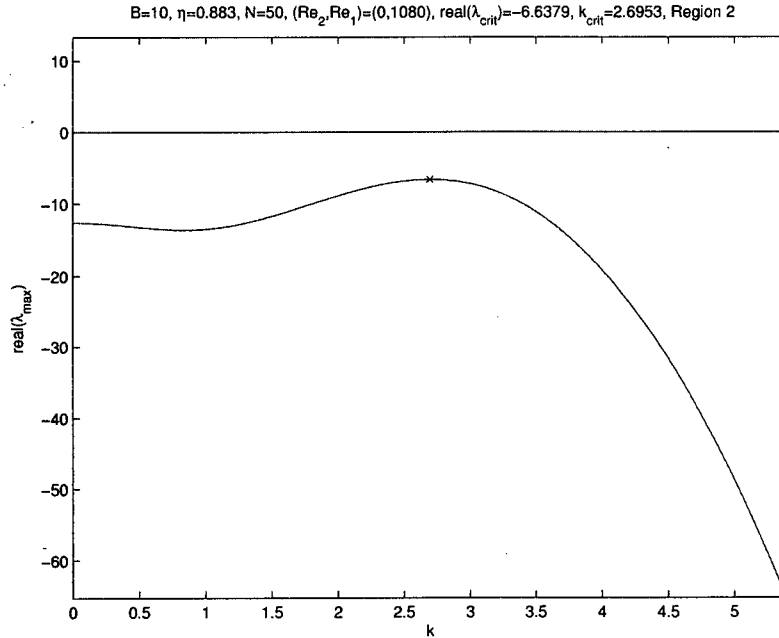


Figure 4.1:  $Re_1$  is too small. Instability has not yet occurred.

If  $real(\lambda_{crit}(Re_1, Re_2, k_{crit})) < 0$  then the perturbation will decay with time, so that  $Re_1$  is too small and the instability has not occurred yet in the system. Similarly, if  $real(\lambda_{crit}(Re_1, Re_2, k_{crit})) > 0$  then the perturbation will grow with time, so that  $Re_1$  is too large and the instability has already occurred for some smaller value of  $Re_1$ .

For example, suppose we choose the set of values  $B = 10$ ,  $\eta = 0.883$ ,  $Re_2 = 0$  with an initial guess of  $Re_1 = 1080$ . Figure 4.1 shows that  $real(\lambda_{crit}) < 0$  so that we need to increase  $Re_1$ . As a second attempt, we guess a larger value for  $Re_1$ , say  $Re_1 = 1180$ . Figure 4.2 shows that  $real(\lambda_{crit}) > 0$  so that  $Re_1$  is too large. Finally, choosing  $Re_1 = 1131.3351$  results in a “small enough” value for  $real(\lambda_{crit})$  as seen in figure 4.3. Finally, we plot the pair of points  $(Re_2, Re_1) = (0, 1131.3351)$ . By continuing in this manner for several values of  $Re_2$ , we obtain the entire marginal stability curve, as seen in figure 4.4 where we use  $N = 50$ . The relative error for  $Re_{1,crit}$  between  $N = 50$  and  $N = 75$  is approximately 0.18 % while the relative error between  $N = 75$  and  $N = 100$  is approximately 0.054 %. Figure 4.5 shows a flowchart for the marginal stability code.

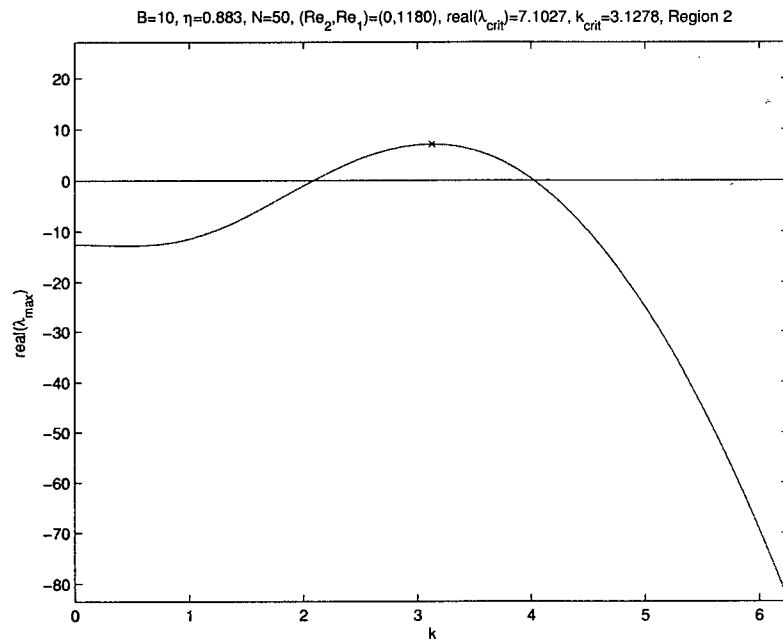


Figure 4.2:  $Re_1$  is too large. Instability has already occurred.

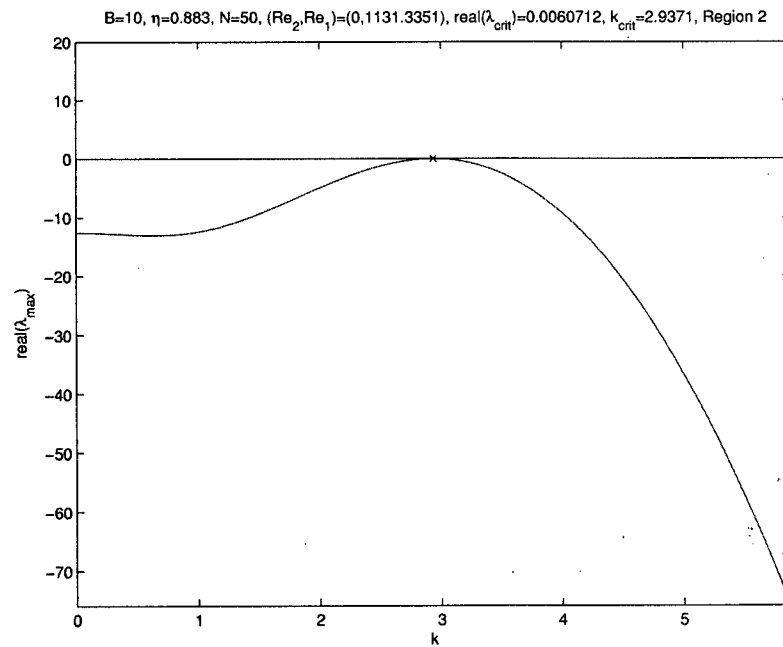


Figure 4.3:  $Re_1 = Re_{1crit}$

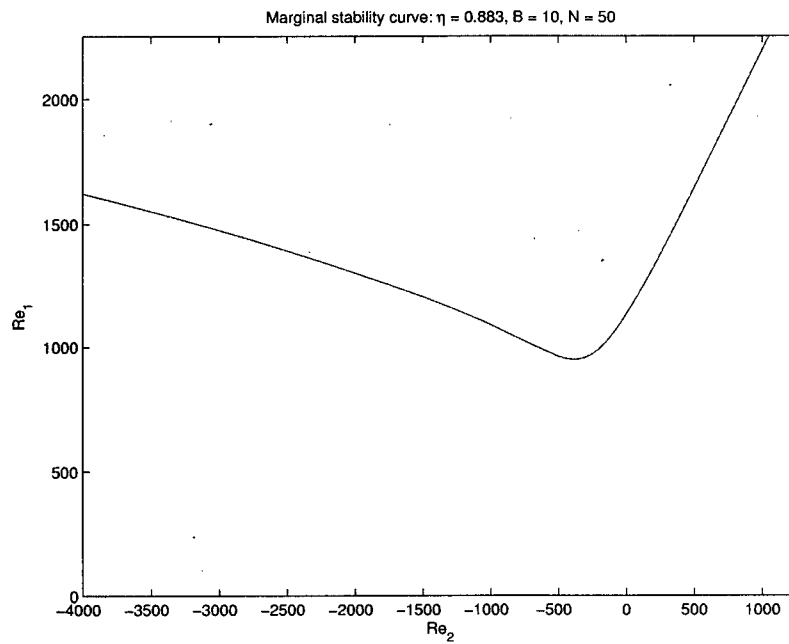


Figure 4.4: Marginal stability curve for  $B = 10, \eta = 0.883$

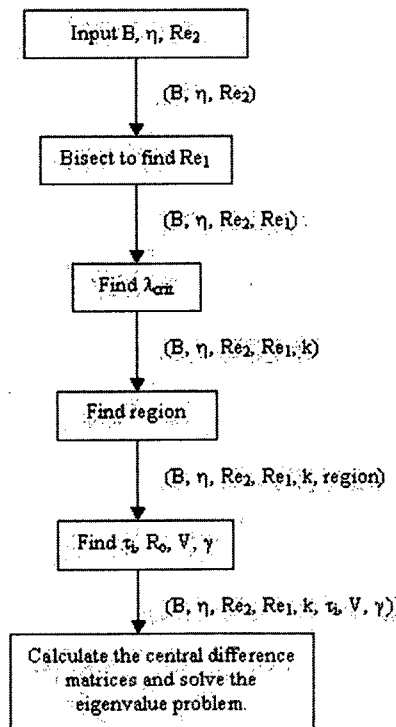


Figure 4.5: Flowchart of marginal stability code

# Chapter 5

## Results for an Axisymmetric Disturbance

### 5.1 Numerical Results

#### 5.1.1 Comparison with Newtonian Results

Our first goal was to reproduce the marginal stability curve for the linear instability of a Newtonian fluid. We were able to compare our curve for  $m = 0$ ,  $\eta = 0.883$ ,  $B = 0$  with the linear instability curve in [9] courtesy of Dr. Randall Tagg from the University of Colorado in Denver who provided us with the numerical data. From figure 5.1 we can see that our numerical results are in agreement.

#### 5.1.2 Results for $B > 0$

We will first begin by looking at results for a narrow gap with  $\eta = 0.883$ . Figure 5.2 shows marginal stability curves for  $B = 1$ ,  $B = 10$ ,  $B = 20$  and  $B = 100$  versus the region as dictated by  $\eta$ ,  $Re_1$ ,  $Re_2$  and  $B$ . Note that above the marginal stability curve, the partial plug and no plug regions may change due to the instability.

We can see clearly in figure 5.3 that as  $B$  increases, the system becomes more stable so that the yield stress acts as a stabilizing agent in the system. This result is in agreement with that of Graebel [8].

In figure 5.4 we plot the critical values of  $Re_1$ , denoted by  $Re_{1_{crit}}$ , versus  $B$  for different values of  $Re_2$ . We can see that  $Re_{1_{crit}}$  is an increasing function of  $B$  for a fixed value of  $Re_2$ . Furthermore, this figure shows that as  $B \rightarrow \infty$ ,  $Re_{1_{crit}}$  becomes progressively independent of  $Re_2$ . That is,

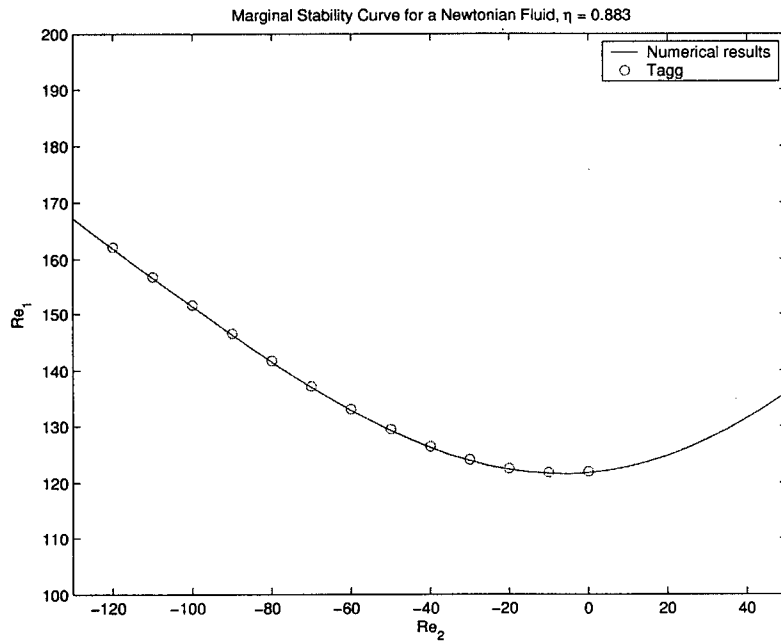


Figure 5.1: Comparison of our numerical calculations against data from [1] for  $m = 0$ .

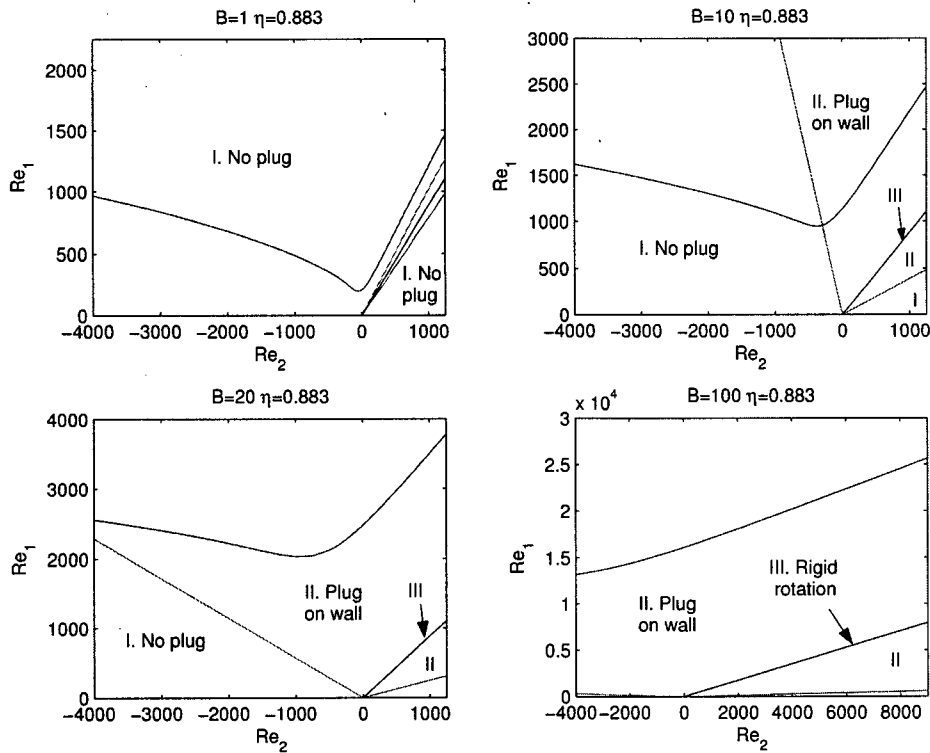
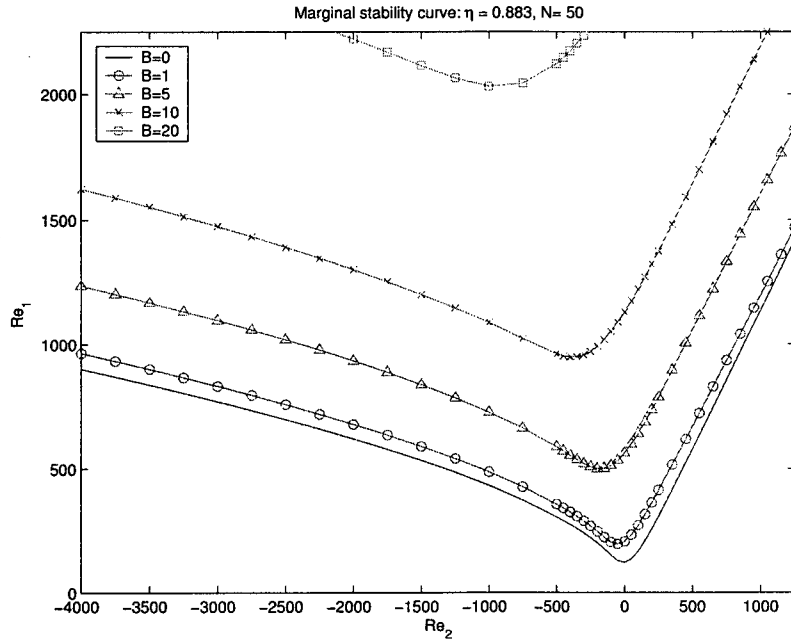


Figure 5.2: Marginal stability curves versus regions for  $\eta = 0.883$  with  $N = 50$ .


 Figure 5.3: Marginal stability curves  $\eta = 0.883$  and varying  $B$ .

$Re_{1_{crit}}$  becomes nearly constant as  $B \rightarrow \infty$ . For large  $B$ , we may assume a solution of the form

$$Re_{1_{crit}} \sim aB^q \quad (5.1)$$

and use a least squares approximation to solve for  $a$  and  $q$ . Only considering values of  $B \geq 200$  and with  $\eta = 0.883$  we get  $a \approx e^{4.0467}$  and  $q \approx 1.2169$ . Figure 5.5 shows the approximation (5.1) along with a plot for  $Re_{1_{crit}}$  when  $B = 1000$ . The dependency of  $Re_{1_{crit}}$  on  $Re_2$  is clearly much weaker than with respect to  $B$ . Table 5.1 shows approximate values of  $a$  and  $q$  for different values of  $\eta$ .

We now wish to see if this result holds for flows with a wider gap. As seen in figure 5.6, for a gap width of  $\eta = 0.5$ ,  $Re_{1_{crit}}$  still becomes progressively independent of  $Re_2$  for large  $B$ . However, we note that  $Re_{1_{crit}}$  is not necessarily an increasing function of  $B$ . For example, the curve with  $Re_2 = 1000$  shows that  $Re_{1_{crit}}$  first decreases from  $B = 0$  and then increases again at around  $B = 2$ . Therefore, for a wider gap, the presence of a yield stress is not necessarily

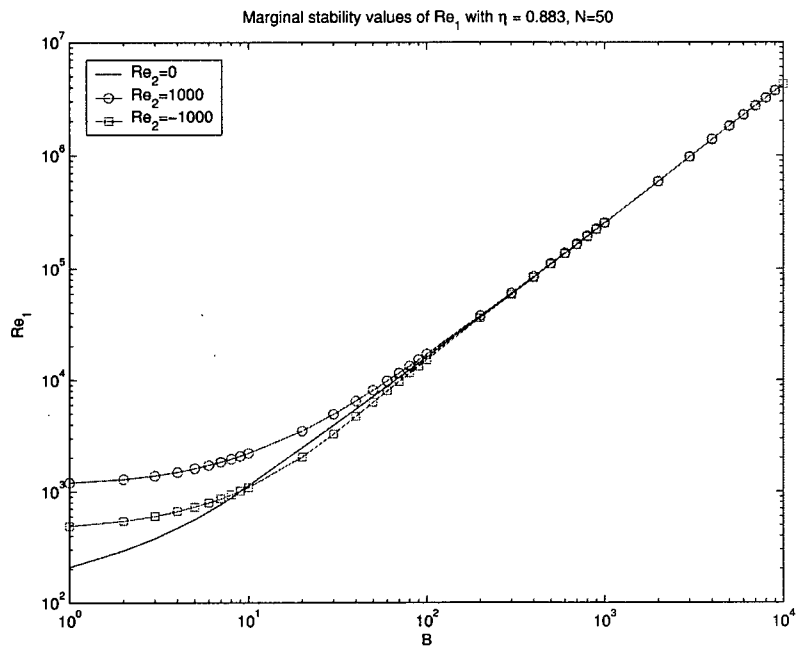


Figure 5.4:  $Re_{1,crit}$  becomes progressively independent of  $Re_2$  as  $B$  increases.

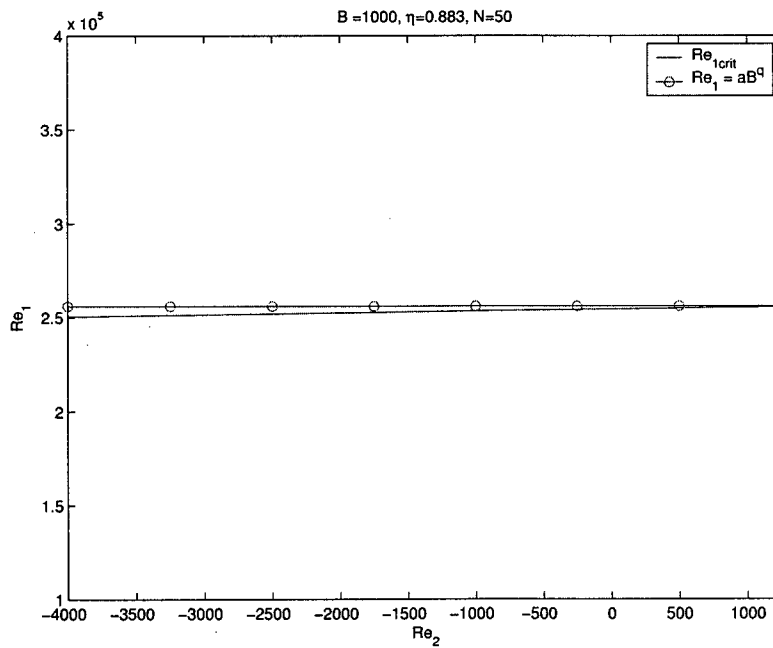


Figure 5.5:  $Re_{1,crit}$  for  $B = 1000$  with the asymptotic solution  $Re_{1,crit} = aB^q$ ;  $a = e^{4.0467}$ ,  $q = 1.2169$ .

$\eta$	$a$	$q$
0.3	$e^{3.8687}$	1.1619
0.5	$e^{3.7996}$	1.1946
0.75	$e^{3.9206}$	1.2076
0.883	$e^{4.0467}$	1.2169

Table 5.1: Approximate least squares values for  $a$  and  $q$  for  $B \geq 200$  with  $N = 50$ .

a stabilizing factor in the flow. In fact, we see that for certain values of  $B$  it may destabilize the system. Figure 5.7 shows curves for  $\eta = 0.5$  and various values of  $B$ . We can see that for  $Re_2 > 0$ , some values of  $B$  are more destabilizing than others, but there is no obvious pattern. However, the yield stress is still a stabilizing factor for  $Re_2 < 0$ .

In figure 5.7 we note also that the rigid rotation line  $Re_1 = \eta Re_2$  acts as a lower bound for stability. We will show in section 5.3 that this lower bound holds for all values of  $B$  and  $\eta$ . Intuitively, when the entire region between the two cylinders moves in rigid rotation, we do not expect any instabilities to occur.

## 5.2 Heuristic Results

In this section we will apply Rayleigh's criterion for an inviscid flow to our velocity profile for a Bingham fluid. Rayleigh's criterion gives a lower estimate for stability using physical arguments. Firstly, we will give a brief outline of Rayleigh's argument.

Euler's equation for an inviscid flow in dimensional variables is given by

$$\hat{\rho} \left( \frac{\partial \hat{\mathbf{U}}}{\partial \hat{t}} + (\hat{\mathbf{U}} \cdot \hat{\nabla}) \hat{\mathbf{U}} \right) = -\hat{\nabla} \hat{P} \quad (5.2)$$

where  $\hat{\mathbf{U}} = \hat{U} \mathbf{e}_r + \hat{V} \mathbf{e}_\theta + \hat{W} \mathbf{e}_z$ . Assuming an azimuthal axisymmetric flow gives the  $\theta$  component

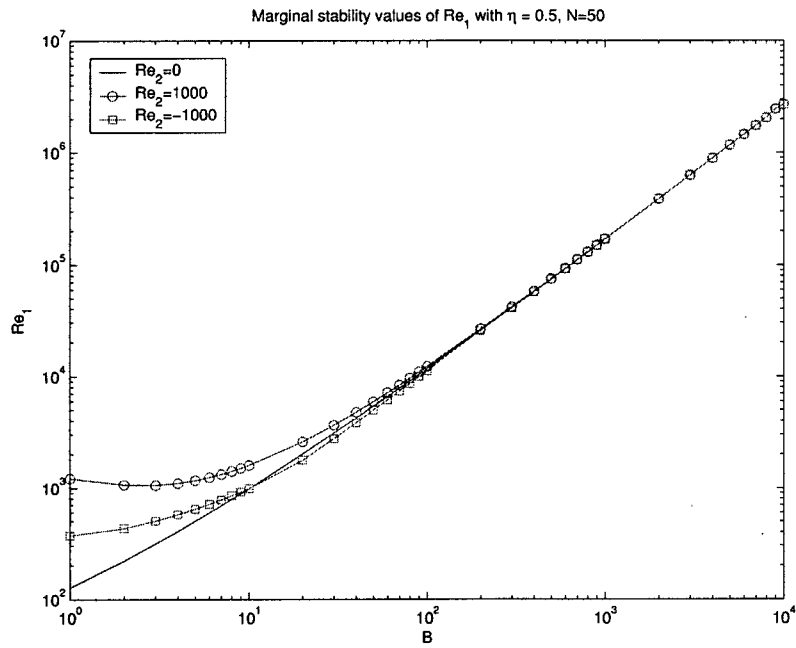


Figure 5.6: For a larger gap,  $Re_{1,crit}$  is not necessarily an increasing function of  $B$ .

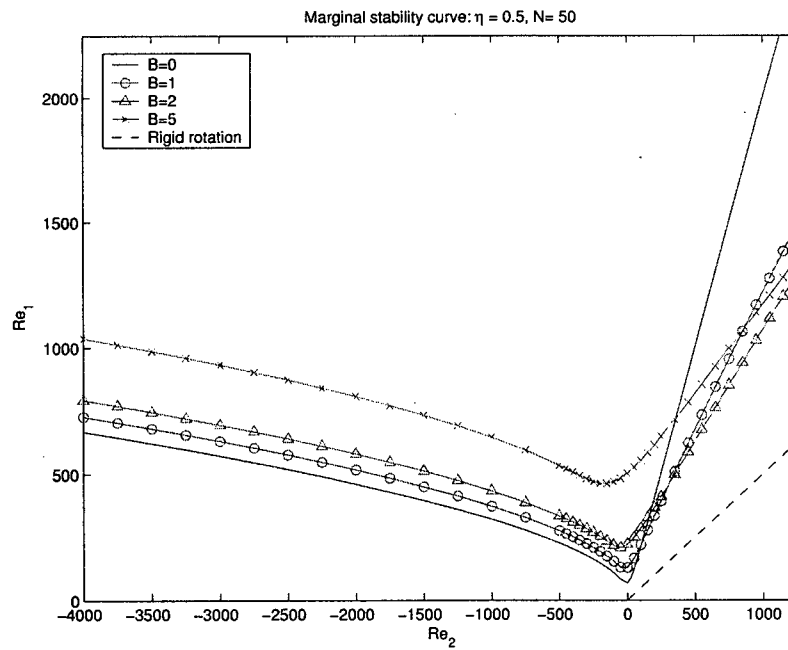


Figure 5.7: Marginal stability curves with  $\eta = 0.5$  and varying  $B$ .

$$\frac{\partial \hat{V}}{\partial \hat{t}} + \hat{U} \frac{\partial \hat{V}}{\partial \hat{r}} + \frac{\hat{U} \hat{V}}{\hat{r}} + \hat{W} \frac{\partial \hat{V}}{\partial \hat{z}} = 0 \quad (5.3)$$

which can be rewritten as

$$\frac{D(\hat{r}\hat{V})}{D\hat{t}} = 0 \quad (5.4)$$

where  $\frac{D}{D\hat{t}}$  is the material derivative. It follows from equation (5.4) that angular momentum is conserved for an inviscid fluid. Let us return to our dimensionless equations. Now, consider two small fluid elements, one located at  $r_1$  and one located at  $r_2$  with  $R_1 < r_1 < r_2 < R_0$ . Suppose that the fluid element at  $r_1$  moves up to position  $r_2$ . Then, according to the conservation of angular momentum, its velocity at  $r_2$  is given by

$$V(r_2) = \frac{r_1 V(r_1)}{r_2}. \quad (5.5)$$

According to the  $r$ -momentum equation (2.3), the local pressure gradient at  $r = r_2$  is given by

$$\frac{\partial P(r_2)}{\partial r} = Re_1 \frac{(V(r_2))^2}{r_2}. \quad (5.6)$$

In order for the fluid element to return to its position  $r_1$ , we must have

$$Re_1 \frac{(V(r_2))^2}{r_2} > Re_1 \frac{(r_1 V(r_1))^2}{r_2} \quad (5.7)$$

which can be expressed as

$$(r_2 V(r_2))^2 > (r_1 V(r_1))^2. \quad (5.8)$$

That is, we will have stability when

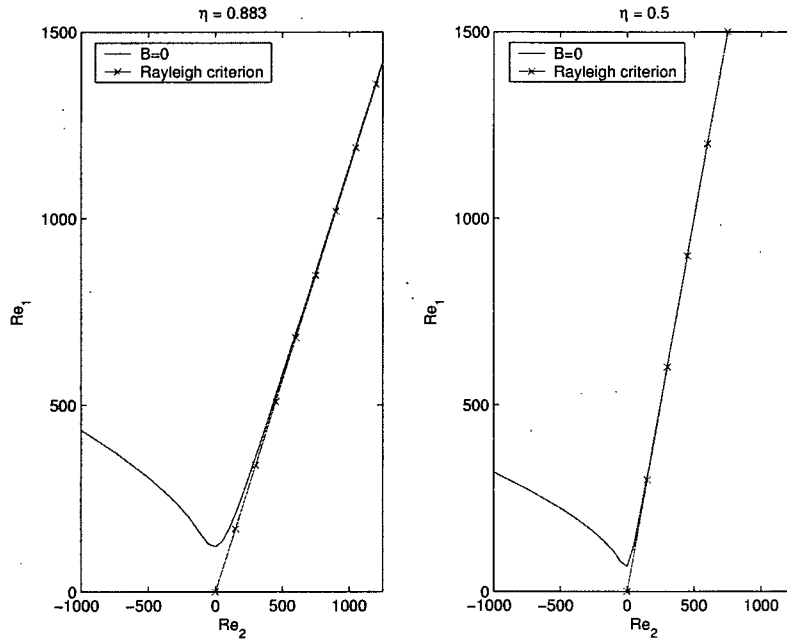


Figure 5.8: Marginal stability curve for a Newtonian fluid along with the Rayleigh criterion.

$$\frac{d(rV)^2}{dr} > 0. \quad (5.9)$$

Equation (5.9) is known as Rayleigh's criterion for an inviscid fluid [10]. It follows from this criterion that for a Newtonian fluid in Couette flow, the flow will be stable when  $\Omega > \eta^2$  or

$$Re_1 < \frac{Re_2}{\eta}. \quad (5.10)$$

This analysis is not rigorous, but from figure 5.8 we see that the marginal stability curve for a Newtonian fluid asymptotically approaches the Rayleigh criterion as  $Re_2 \rightarrow \infty$ .

Let us now apply the Rayleigh criterion to our velocity profile for a Bingham fluid. Again, this method will not be rigorous, but should indicate when the velocity profile has a tendency to be stable, neglecting viscous effects. It follows from equation (5.9) that stability occurs if

$$2(r^2\omega(r))\frac{d(Vr)}{dr} > 0 \quad (5.11)$$

where  $\omega(r) = V/r$  is the angular speed at any point  $r$  in the flow. We will assume that  $\hat{\Omega}_2 > 0$ . It follows that  $\omega(r) > 0$  so that stability occurs wherever  $\frac{d(Vr)}{dr} > 0$ . Assuming that  $\tau_i < -B$  we obtain

$$\frac{d(Vr)}{dr} = 2A_1r + Br(1 + 2\ln(r)) > 2A_1r + Br(1 + 2\ln(R_1)). \quad (5.12)$$

Therefore, our stability criterion becomes

$$2A_1 + B(1 + 2\ln(R_1)) > 0 \quad (5.13)$$

where

$$A_1 = \frac{\Omega}{R_1} + \frac{\tau_i R_1^2}{2R_o^2} - B \ln(R_o). \quad (5.14)$$

In figure 5.9 we plot the above criterion and note that the rigid rotation is always stable. In fact, Rayleigh's criterion for large  $B$  and the rigid rotation criterion almost coincide. This result also implies that whenever  $\tau_i > 0$ , the flow will be stable. When  $B = 0$  we obtain the Raleigh criterion for a Newtonian fluid.

### 5.3 A Lower Bound for Stability

The preceding analysis of the Rayleigh criterion indicates that the rigid rotation curve is always stable, and this result is also confirmed by our numerical results. Furthermore, intuitively we expect that when the cylinders are locked ( $\Omega = 1$ ) an infinitesimal perturbation will be unable to break the unyielded fluid. In this section, we demonstrate that the above information is correct by deriving a rigorous bound for linear stability.

We will show that  $\text{real}(\lambda) < 0$  if the inequality

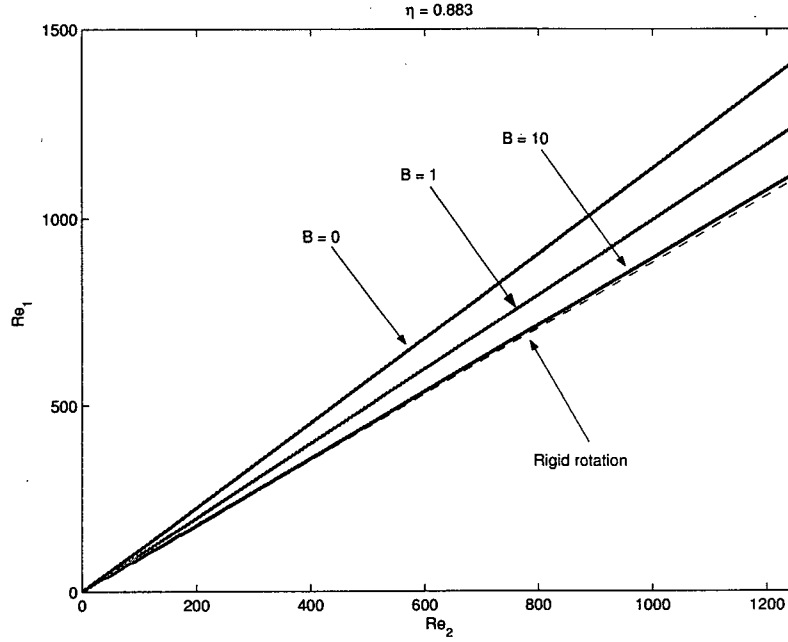


Figure 5.9: Solid lines: Rayleigh criterion. Dashed line: Rigid rotation  $Re_1 = \eta Re_2$ ;  $\eta = 0.883$ .

$$\frac{Re_1}{2} \dot{\gamma}_{max} \left( \frac{R_o}{R_1} \right)^{\frac{1}{2}} (R_o - R_1) - \min \left\{ 1, \frac{R_1}{R_2} \pi^2 \right\} \left( 1 + \frac{B}{\dot{\gamma}_{max}} \right) < 0 \quad (5.15)$$

holds. This inequality is a sufficient but not necessary condition for linear stability. It serves as a conservative approximation for linear stability.

We will proceed as in [7]. Let  $\bar{u}$ ,  $\bar{v}$  and  $\bar{w}$  be the complex conjugates of  $u$ ,  $v$  and  $w$  respectively. To begin the derivation of equation (5.15) we multiply equation (4.1) by  $r\bar{u}$ , (4.2) by  $r\bar{v}$ , (4.3) by  $r\bar{w}$  and integrate from  $R_1$  to  $R_o$  to obtain

$$\begin{aligned} \lambda \int_{R_1}^{R_o} r u \bar{u} dr &= 2Re_1 \int_{R_1}^{R_o} V v \bar{u} dr - \int_{R_1}^{R_o} r \bar{u} D p dr \\ &+ \int_{R_1}^{R_o} \left( r \bar{u} D^2 u + \bar{u} D u - k^2 r \bar{u} u - \frac{\bar{u} u}{r} \right) dr \\ &+ B \int_{R_1}^{R_o} r \bar{u} \phi_r dr \end{aligned} \quad (5.16)$$

$$\begin{aligned}
 \lambda \int_{R_1}^{R_o} r \bar{v} v \, dr &= -Re_1 \int_{R_1}^{R_o} (r DV + V) \bar{v} u \, dr \\
 &+ \int_{R_1}^{R_o} \left( r \bar{v} D^2 v + \bar{v} Dv - k^2 r \bar{v} v - \frac{\bar{v} v}{r} \right) \\
 &- k^2 B \int_{R_1}^{R_o} \frac{r \bar{v} v}{\dot{\gamma}} \, dr
 \end{aligned} \tag{5.17}$$

$$\begin{aligned}
 \lambda \int_{R_1}^{R_o} r \bar{w} w \, dr &= -ik \int_{R_1}^{R_o} r \bar{w} p \, dr \\
 &+ \int_{R_1}^{R_o} (r \bar{w} D^2 w + \bar{w} Dw - k^2 r \bar{w} w) \, dr \\
 &+ B \int_{R_1}^{R_o} r \bar{w} \phi_z \, dr.
 \end{aligned} \tag{5.18}$$

Add equations (5.16) - (5.18) to obtain

$$\lambda \|\mathbf{u}\|^2 = Re_1 I_{inertial} - I_{viscous} - BI_{Bingham} \tag{5.19}$$

where

$$\|\mathbf{u}\|^2 = \int_{R_1}^{R_o} r (|u|^2 + |v|^2 + |w|^2) \, dr \tag{5.20}$$

$$I_{inertial} = \int_{R_1}^{R_o} \left( 2Vv\bar{u} - r \left( DV - \frac{V}{r} \right) \bar{v}u \right) \, dr \tag{5.21}$$

$$I_{Bingham} = - \int_{R_1}^{R_o} \left( r \bar{u} \phi_r - k^2 r \frac{|v|^2}{\dot{\gamma}} + r \bar{w} \phi_z \right) \, dr \tag{5.22}$$

and

$$I_{viscous} = I_1 + I_2 \quad (5.23)$$

with

$$I_1 = \int_{R_1}^{R_o} (r\bar{u}Dp + ikr\bar{w}p) dr \quad (5.24)$$

$$\begin{aligned} I_2 = & - \int_{R_1}^{R_o} \left( r\bar{u}D^2u + \bar{u}Du - k^2r|u|^2 - \frac{|u|^2}{r} \right) dr \\ & - \int_{R_1}^{R_o} \left( r\bar{v}D^2v + \bar{v}Dv - k^2r|v|^2 - \frac{|v|^2}{r} \right) dr \\ & - \int_{R_1}^{R_o} \left( r\bar{w}D^2w + \bar{w}Dw - k^2r|w|^2 \right) dr. \end{aligned} \quad (5.25)$$

We will proceed to simplify the integrals  $I_{inertial}$ ,  $I_{viscous}$  and  $I_{Bingham}$  using integration by parts and applying the boundary conditions (3.60) with  $m = 0$ . Then we will proceed to bound these integrals using the Cauchy-Schwarz and triangle inequalities. Finally, we will apply the Poincaré inequality to find our conservative estimate.

### 5.3.1 Simplifying the Integrals

We will show that both of the integrals  $I_{viscous}$  and  $I_{Bingham}$  are real and positive, while the integral  $I_{inertia}$  is complex. Of interest is the real part of equation (5.19) because we would like to determine the condition for which  $\text{real}(\lambda) < 0$ . Note that  $I_1 = 0$  since by the continuity equation (4.4) and by integration by parts

$$\begin{aligned} I_1 &= \int_{R_1}^{R_o} \left( r\bar{u}Dp + r \left( D\bar{u} + \frac{\bar{u}}{r} \right) p \right) dr \\ &= - \int_{R_1}^{R_o} (rD\bar{u} + \bar{u})p dr + \int_{R_1}^{R_o} r \left( D\bar{u} + \frac{\bar{u}}{r} \right) p dr = 0. \end{aligned} \quad (5.26)$$

We can rewrite  $I_2$  as

$$I_2 = k^2 \int_{R_1}^{R_o} r |\mathbf{u}|^2 dr + \int_{R_1}^{R_o} \left( \frac{|u|^2 + |v|^2}{r} \right) dr - I_{21} - I_{22} \quad (5.27)$$

where

$$I_{21} = \int_{R_1}^{R_o} (r\bar{u}D^2u + r\bar{v}D^2v + r\bar{w}D^2w) dr \quad (5.28)$$

and

$$I_{22} = \int_{R_1}^{R_o} (\bar{u}Du + \bar{v}Dv + \bar{w}Dw) dr. \quad (5.29)$$

Using integration by parts, we see that

$$\begin{aligned} I_{21} &= [(r\bar{u})Du + (r\bar{v})Dv + (r\bar{w})Dw]_{R_1}^{R_o} \\ &\quad - \int_{R_1}^{R_o} (D(r\bar{u})Du + D(r\bar{v})Dv + D(r\bar{w})Dw) dr \\ &= - \int_{R_1}^{R_o} r(|Du|^2 + |Dv|^2 + |Dw|^2) dr \\ &\quad - \int_{R_1}^{R_o} (\bar{u}Du + \bar{v}Dv + \bar{w}Dw) dr \\ &= - \int_{R_1}^{R_o} r|D\mathbf{u}|^2 dr - I_{22} \end{aligned} \quad (5.30)$$

so that integral  $I_{viscous}$  becomes

$$I_{viscous} = \int_{R_1}^{R_o} \left( r|D\mathbf{u}|^2 + k^2r|\mathbf{u}|^2 + \frac{|u|^2 + |v|^2}{r} \right) dr. \quad (5.31)$$

Let us rewrite the Bingham integral  $I_{Bingham}$ . Integrating by parts we obtain

$$\begin{aligned}
 \int_{R_1}^{R_o} r\bar{u}\phi_r dr &= \int_{R_1}^{R_o} \left( \bar{u}D \left( \frac{2rDu}{\dot{\gamma}} \right) + \frac{r\bar{u}}{\dot{\gamma}} \left( ikDw - \left( k^2 + \frac{2}{r^2} \right) u \right) \right) dr \\
 &= \left[ \bar{u} \left( \frac{2rDu}{\dot{\gamma}} \right) \right]_{R_1}^{R_o} - \int_{R_1}^{R_o} D\bar{u} \left( \frac{2rDu}{\dot{\gamma}} \right) dr \\
 &\quad + \int_{R_1}^{R_o} \frac{r\bar{u}}{\dot{\gamma}} \left( ikDw - \left( k^2 + \frac{2}{r^2} \right) u \right) dr.
 \end{aligned} \tag{5.32}$$

Note that if  $R_o = R_y$  then it follows from the boundary conditions (3.60) with  $m = 0$  that

$$\lim_{r \rightarrow R_y} \frac{2rDu}{\dot{\gamma}} = \lim_{r \rightarrow R_y} \frac{2(rD^2u + Du)}{D\dot{\gamma}} = \frac{0}{D\dot{\gamma}(R_y)} = 0 \tag{5.33}$$

so that

$$\left[ \bar{u} \left( \frac{2rDu}{\dot{\gamma}} \right) \right]_{R_1}^{R_o} = 0 \tag{5.34}$$

and we obtain

$$\int_{R_1}^{R_o} r\bar{u}\phi_r dr = - \int_{R_1}^{R_o} \frac{1}{\dot{\gamma}} \left( 2r|Du|^2 + r \left( k^2 + \frac{2}{r^2} \right) |u|^2 - ikr\bar{u}Dw \right) dr. \tag{5.35}$$

Through similar methods, we obtain

$$\begin{aligned}
 \int_{R_1}^{R_o} r\bar{w}\phi_z &= \int_{R_1}^{R_o} \left( \bar{w}D \left( r \frac{(iku + Dw)}{\dot{\gamma}} \right) - \frac{2rk^2}{\dot{\gamma}} |w|^2 \right) dr \\
 &= \left[ \bar{w} \left( r \frac{iku + Dw}{\dot{\gamma}} \right) \right]_{R_1}^{R_o} - \int_{R_1}^{R_o} \frac{r}{\dot{\gamma}} (D\bar{w}(iku + Dw) + 2k^2|w|^2) dr \\
 &= - \int_{R_1}^{R_o} \frac{r}{\dot{\gamma}} (ikuD\bar{w} + |Dw|^2 + 2k^2|w|^2) dr.
 \end{aligned} \tag{5.36}$$

The Bingham integral becomes

$$I_{Bingham} = \int_{R_1}^{R_o} \frac{1}{\dot{\gamma}} \left( 2 \left( r |Du|^2 + \frac{|u|^2}{r} \right) + rk^2(|v|^2 + 2|w|^2) + r|x|^2 \right) dr \quad (5.37)$$

where

$$x = ku - iDw. \quad (5.38)$$

Note that both  $I_{viscous}$  and  $I_{Bingham}$  are real and positive, which implies that the imaginary part of  $\lambda$  can only come from the inertial integral  $I_{inertia}$ . Let us proceed by only considering the real part of equation (5.19). First, define the following quantities

$$v = v_R + iv_I \quad (5.39)$$

$$u = u_R + iu_I. \quad (5.40)$$

We can rewrite the integrand of  $I_{inertia}$  as

$$\begin{aligned} 2Vv\bar{u} - r \left( DV - \frac{V}{r} \right) \bar{v}u &= 2V(v\bar{u} - \bar{v}u) - (rDV - V)\bar{v}u \\ &= -r\dot{\gamma}_{r\theta}(u_Rv_R + u_Iv_I) + i(4V + r\dot{\gamma}_{r\theta})(v_Iu_R - v_Ru_I) \end{aligned} \quad (5.41)$$

so that

$$\text{real}(I_{inertia}) = \int_{R_1}^{R_o} r(-\dot{\gamma}_{r\theta})(u_Rv_R + u_Iv_I) dr. \quad (5.42)$$

### 5.3.2 Bounding the Integrals

We will begin by bounding  $\text{real}(I_{inertia})$ . First note that

$$\begin{aligned} \text{real}(I_{inertia}) &\leq \int_{R_1}^{R_o} r |\dot{\gamma}_{r\theta}| (|u_R| |v_R| + |u_I| |v_I|) dr \\ &\leq \dot{\gamma}_{max} \int_{R_1}^{R_o} r (|u_R| |v_R| + |u_I| |v_I|) dr. \end{aligned} \quad (5.43)$$

We can now apply a bound to the integrals of both  $r|u_R||v_R|$  and  $r|u_I||v_I|$  as follows. Rewrite the integral of  $r|u_R||v_R|$  as

$$\begin{aligned} \int_{R_1}^{R_o} r |u_R| |v_R| dr &= \int_{R_1}^{R_o} |v_R| \left| \int_{R_1}^r D(yu_R(y)) dy \right| dr \\ &\leq \int_{R_1}^{R_o} |v_R| \left( \int_{R_1}^r |D(yu_R(y))| dy \right) dr \\ &= \int_{R_1}^{R_o} |v_R| \left( \int_{R_1}^r |kyw_I| dy \right) dr \\ &\leq k \int_{R_1}^{R_o} |v_R| \left( \int_{R_1}^{R_o} |yw_I| dy \right) dr \\ &= k \int_{R_1}^{R_o} |v_R| dr \int_{R_1}^{R_o} |rw_I| dr \\ &\leq k \int_{R_1}^{R_o} \left( \frac{r}{R_1} \right)^{\frac{1}{2}} |v_R| dr \int_{R_1}^{R_o} R_o^{\frac{1}{2}} r^{\frac{1}{2}} |w_I| dr \\ &= k \left( \frac{R_o}{R_1} \right)^{\frac{1}{2}} \int_{R_1}^{R_o} r^{\frac{1}{2}} |v_R| dr \int_{R_1}^{R_o} r^{\frac{1}{2}} |w_I| dr. \end{aligned} \quad (5.44)$$

Using the Cauchy-Schwarz inequality with the inner product

$$\langle f, g \rangle = \int_{R_1}^{R_o} f(r)g(r)dr \quad (5.45)$$

gives

$$\langle 1, r^{\frac{1}{2}} |v_R| \rangle \leq \sqrt{\langle 1, 1 \rangle} \sqrt{\langle r^{\frac{1}{2}} |v_R|, r^{\frac{1}{2}} |v_R| \rangle} \quad (5.46)$$

$$\langle 1, r^{\frac{1}{2}} |w_I| \rangle \leq \sqrt{\langle 1, 1 \rangle} \sqrt{\langle r^{\frac{1}{2}} |w_I|, r^{\frac{1}{2}} |w_I| \rangle} \quad (5.47)$$

so that

$$\int_{R_1}^{R_o} r |u_R| |v_R| dr \leq k \left( \frac{R_o}{R_1} \right)^{\frac{1}{2}} (R_o - R_1) \|v_R\| \|w_I\|. \quad (5.48)$$

Similarly, we obtain

$$\int_{R_1}^{R_o} r |u_I| |v_I| dr \leq k \left( \frac{R_o}{R_1} \right)^{\frac{1}{2}} (R_o - R_1) \|v_I\| \|w_R\|. \quad (5.49)$$

We can rewrite equation (5.43) as

$$\begin{aligned} \text{real}(I_{inertia}) &\leq \dot{\gamma}_{max} \left( \frac{R_o}{R_1} \right)^{\frac{1}{2}} (R_o - R_1) (k \|v_R\| \|w_I\| + k \|v_I\| \|w_R\|) \\ &\leq \dot{\gamma}_{max} \left( \frac{R_o}{R_1} \right)^{\frac{1}{2}} (R_o - R_1) \left( \frac{k^2 \|v_R\|^2 + \|w_I\|^2}{2} + \frac{k^2 \|v_I\|^2 + \|w_R\|^2}{2} \right) \\ &= \frac{1}{2} \dot{\gamma}_{max} \left( \frac{R_o}{R_1} \right)^{\frac{1}{2}} (R_o - R_1) (k^2 \|v\|^2 + \|w\|^2). \end{aligned} \quad (5.50)$$

From inequality (5.50), it follows that we need to bound  $I_{Bingham}$  and  $I_{viscous}$  below with the integrals  $k^2 \|v\|^2$  and  $\|w\|^2$ . In order to bound  $I_{Bingham}$ , we first set

$$I_{Bingham} \geq \frac{B}{\dot{\gamma}_{max}} \int_{R_1}^{R_o} \left( 2 \left( r |Du|^2 + \frac{|u|^2}{r} \right) + rk^2 (|v|^2 + 2|w|^2) + r|x|^2 \right) dr. \quad (5.51)$$

Note that  $|x|^2 = k^2 |u|^2 + ik(uD\bar{w} - \bar{u}Dw) + |Dw|^2$ . Applying the continuity equation to the  $ikr(\bar{u}Dw - uD\bar{w})$  term in the above integral, and integrating it by parts gives

$$ik \int_{R_1}^{R_o} ((ru)D\bar{w} - (r\bar{u})Dw) dr = - \int_{R_1}^{R_o} 2 \left( r |Du|^2 + \frac{|u|^2}{r} \right) dr. \quad (5.52)$$

Therefore,

$$\begin{aligned}
 I_{Bingham} &\geq \frac{B}{\dot{\gamma}_{max}} \int_{R_1}^{R_o} (k^2 r (|v|^2 + 2|w|^2) + k^2 r |u|^2 + r |Dw|^2) dr \\
 &\geq \frac{B}{\dot{\gamma}_{max}} \int_{R_1}^{R_o} (k^2 r |v|^2 + r |Dw|^2) dr.
 \end{aligned} \tag{5.53}$$

The final and simplest integral to bound is  $I_{viscous}$  and we set

$$I_{viscous} \geq \int_{R_1}^{R_o} (k^2 r |v|^2 + r |Dw|^2) dr. \tag{5.54}$$

From the inequalities (5.50), (5.53) and (5.54) it follows that

$$\lambda_R \|\mathbf{u}\|^2 \leq \frac{Re_1}{2} \dot{\gamma}_{max} \left( \frac{R_o}{R_1} \right)^{\frac{1}{2}} (R_o - R_1) (k^2 \|v\|^2 + \|w\|^2) - \left( 1 + \frac{B}{\dot{\gamma}_{max}} \right) (k^2 \|v\|^2 + \|Dw\|^2). \tag{5.55}$$

### 5.3.3 Applying the Poincaré Inequality

We now need to find a lower bound for  $\|Dw\|^2$  involving  $\|w\|^2$ . It follows from the Poincaré inequality that

$$\int_0^1 \left| \frac{dw}{dy} \right|^2 dy \geq \pi^2 \int_0^1 |w|^2 dy. \tag{5.56}$$

Introduce a change of variable  $r = R_1 + (R_o - R_1)y$ . Then we obtain

$$\begin{aligned}
 \int_{R_1}^{R_o} \left| \frac{dw}{dr} \right|^2 dr &= \frac{1}{R_o - R_1} \int_0^1 \left| \frac{dw}{dy} \right|^2 dy \\
 &\geq \frac{\pi^2}{R_o - R_1} \int_0^1 |w|^2 dy \\
 &= \frac{\pi^2}{(R_o - R_1)^2} \int_{R_1}^{R_o} |w|^2 dr.
 \end{aligned} \tag{5.57}$$

Therefore

$$\int_{R_1}^{R_o} r |Dw|^2 dr \geq R_1 \int_{R_1}^{R_o} |Dw|^2 dr \quad (5.58)$$

$$\begin{aligned} &\geq R_1 \frac{\pi^2}{(R_o - R_1)^2} \int_{R_1}^{R_o} |w|^2 dr \\ &\geq R_1 \frac{\pi^2}{(R_o - R_1)^2} \int_{R_1}^{R_o} \frac{r}{R_o} |w|^2 dr \\ &\geq \frac{R_1}{R_2} \pi^2 \int_{R_1}^{R_o} r |w|^2 dr \end{aligned} \quad (5.59)$$

$$\geq \min\{1, C\} \int_{R_1}^{R_o} r |w|^2 dr \quad (5.60)$$

where

$$C = \frac{R_1}{R_2} \pi^2. \quad (5.61)$$

Substituting  $\|Dw\|^2 + k^2\|v\|^2 \geq \min\{1, C\}(\|w\|^2 + k^2\|v\|^2)$  into equation (5.55) gives

$$\lambda_R \|\mathbf{u}\|^2 \leq \left( \frac{Re_1}{2} \dot{\gamma}_{max} \left( \frac{R_o}{R_1} \right)^{\frac{1}{2}} (R_o - R_1) - \min\{1, C\} \left( 1 + \frac{B}{\dot{\gamma}_{max}} \right) \right) (k^2\|v\|^2 + \|w\|^2) \quad (5.62)$$

so that we will have stability when  $\lambda_R < 0$  or whenever equation (5.15) holds.

### 5.3.4 Results

Let

$$f(Re_1, Re_2) = \frac{Re_1}{2} \dot{\gamma}_{max} \left( \frac{R_o}{R_1} \right)^{\frac{1}{2}} (R_o - R_1) - \min \left\{ 1, \frac{R_1}{R_2} \pi^2 \right\} \left( 1 + \frac{B}{\dot{\gamma}_{max}} \right). \quad (5.63)$$

The plot of  $f(Re_1, Re_2) = 0$  is shown in figure 5.10 for  $B = 10$  and  $B = 100$ . We can see that the rigid rotation line  $Re_1 = \eta Re_2$  is contained inside this contour, so that analytically we have proven that the rigid rotation is stable.

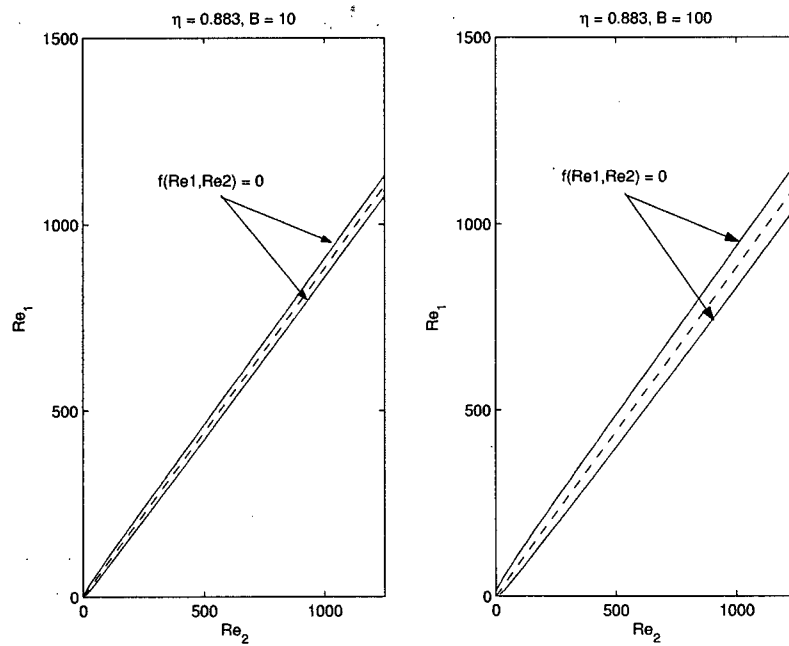


Figure 5.10: Solid line:  $f(Re_1, Re_2) = 0$ . Dashed line: Rigid rotation  $Re_1 = \eta Re_2$ ;  $\eta = 0.883$ .

# Chapter 6

## Conclusions

Using finite difference methods we were able to determine marginal stability curves for various values of  $B$  and  $\eta$ . In the case of a narrow gap, our results agree with [8] in the sense that the yield stress acts as a stabilizing agent in the flow. As the Bingham number increases, the system becomes more stable. However, in the case of a wider gap, the yield stress can destabilize the flow when  $Re_2 > 0$ .

Regardless of the gap width, we found that as  $B \rightarrow \infty$ , the critical inner cylinder Reynolds number  $Re_{1_{crit}}$  becomes weakly dependent on  $Re_2$ . That is,  $Re_1$  depends primarily on  $B$  and  $\eta$ . Using numerical methods, heuristic arguments and analytical methods, we were able to show that the rigid rotation flow is always stable and acts as a lower bound for stability for any values of  $B$  and  $\eta$ . This result implies that whenever the stress at the inner cylinder is positive or  $\hat{\Omega}_2 > \hat{\Omega}_1$ , the flow will be stable.

Future considerations for this problem could include analysis with the  $m > 0$  case and determination of the partial plug region after the onset of instability.

# Bibliography

- [1] C.D. Andereck, S.S. Liu and Harry L. Swinney. Flow regimes in a circular Couette system with independently rotating cylinders. *J. Fluid Mech.*, **164**, pages 155–183, 1985.
- [2] R. Byron-Bird, G.C. Dai and Barbara J. Yarusso. The Rheology and flow of viscoplastic Materials. *Reviews in Chemical Engineering*, **1**, pages 1–70, 1982.
- [3] S. Chandrasekhar. Hydrodynamic and hydromagnetic stability. *Oxford, Clarendon Press*, 1961.
- [4] P. Chossat and G. Iooss. The Couette-Taylor problem. *Springer-Verlag*, 1994.
- [5] B. Engelmann, R. Hiptmair, R.H.W. Hoppe, G. Mazurkevitch. Numerical simulation of electrorheological fluids based on an extended Bingham model. *Computing and Visualization in Science*, **2**, pages 211–219, 2000.
- [6] I. Frigaard and C. Nouar. On the stability of Poiseuille flow of a Bingham fluid. *J. Fluid Mech.*, **263**, pages 133–150, 1994.
- [7] I. Frigaard and C. Nouar. On three-dimensional linear stability of Poiseuille flow of Bingham fluids. *Physics of Fluids*, **15**, pages 2843–2851, 2003.
- [8] W.P. Graebel. The hydrodynamic stability of a Bingham fluid in Couette flow. *International Symposium on Second Order Effects in Elasticity, Plasticity and Fluid Dynamics, Haifa, Pergamon*, pages 636–649, 1964.
- [9] W. F. Langford, Randall Tagg, Eric J. Kostelich, Harry L. Swinney, and Martin Golubitsky. Primary instabilities and bicriticality in flow between counter-rotating cylinders. *Physics of Fluids*, **31**, pages 776–785, 1988.
- [10] R. Tagg. The Couette-Taylor problem. *Nonlinear Science Today*, **4**, pages 2–25, 1994.
- [11] G.I. Taylor. Stability of a viscous liquid contained between two rotating cylinders. *Phil. Trans. Roy. Soc. London A* **223**, pages 289–343, 1923.

# Appendix A

## Numerical Approximations of the Eigenvalue Problem

We will approximate the derivatives of our eigenfunctions  $u$  and  $v$  by using a finite difference method. Let  $N > 0$  be an integer and divide the interval  $[R_1, R_o]$  into  $N - 1$  subintervals each of length  $h = \frac{R_o - R_1}{N - 1}$  and set  $r_i = R_1 + (i - 1)h$  for  $i = 1, 2, \dots, N$ . The derivatives of  $u$  (or  $v$ ) at any point  $r_i$  will be approximated by the central differences

$$Du_i = \frac{u_{i+1} - u_{i-1}}{2h} \quad (\text{A.1})$$

$$D^2u_i = \frac{u_{i+1} - 2u_i + u_{i-1}}{h^2} \quad (\text{A.2})$$

$$D^3u_i = \frac{\frac{1}{2}u_{i+2} - u_{i+1} + u_{i-1} - \frac{1}{2}u_{i-2}}{h^3} \quad (\text{A.3})$$

$$D^4u_i = \frac{u_{i+2} - 4u_{i+1} + 6u_i - 4u_{i-1} + u_{i-2}}{h^4} \quad (\text{A.4})$$

where  $u_i \approx u(r_i)$  and  $Du_i \approx Du(r_i)$ . The boundary conditions  $u = v = 0$  at  $r = R_1, R_o$  satisfied by the eigenfunctions can be rewritten as

$$u(r_1) = u_1 = 0 \quad (\text{A.5})$$

$$u(r_N) = u_N = 0 \quad (\text{A.6})$$

$$v(r_1) = v_1 = 0 \quad (\text{A.7})$$

$$v(r_N) = v_N = 0 \quad (\text{A.8})$$

while the boundary conditions  $Du = 0$  at  $r = R_1, R_o$  can be approximated as

$$Du(r_1) \approx \frac{u_2 - u_0}{2h} = 0 \quad (\text{A.9})$$

$$Du(r_N) \approx \frac{u_{N+1} - u_{N-1}}{2h} = 0 \quad (\text{A.10})$$

That is

$$u_0 = u_2 \quad (\text{A.11})$$

$$u_{N+1} = u_{N-1} \quad (\text{A.12})$$

Each of the estimated derivatives for  $u$  (A.1)-(A.4) along with the boundary conditions for  $u$  (A.5), (A.6), (A.11) and (A.12) can be expressed as the  $(N-2) \times (N-2)$  matrices

$$D \begin{pmatrix} u_2 \\ u_3 \\ u_4 \\ \vdots \\ u_{N-2} \\ u_{N-1} \end{pmatrix} = \frac{1}{h} \begin{pmatrix} 0 & \frac{1}{2} & 0 & 0 & \cdots & 0 \\ -\frac{1}{2} & 0 & \frac{1}{2} & 0 & \cdots & 0 \\ 0 & -\frac{1}{2} & 0 & \frac{1}{2} & \cdots & 0 \\ & & \ddots & & \ddots & \\ 0 & \cdots & 0 & -\frac{1}{2} & 0 & \frac{1}{2} \\ 0 & \cdots & 0 & 0 & -\frac{1}{2} & 0 \end{pmatrix} \begin{pmatrix} u_2 \\ u_3 \\ u_4 \\ \vdots \\ u_{N-2} \\ u_{N-1} \end{pmatrix} \quad (\text{A.13})$$

$$D^2 \begin{pmatrix} u_2 \\ u_3 \\ u_4 \\ \vdots \\ u_{N-2} \\ u_{N-1} \end{pmatrix} = \frac{1}{h^2} \begin{pmatrix} -2 & 1 & 0 & 0 & \cdots & 0 \\ 1 & -2 & 1 & 0 & \cdots & 0 \\ 0 & 1 & -2 & 1 & \cdots & 0 \\ & & \ddots & & \ddots & \\ 0 & \cdots & 0 & 1 & -2 & 1 \\ 0 & \cdots & 0 & 0 & 1 & -2 \end{pmatrix} \begin{pmatrix} u_2 \\ u_3 \\ u_4 \\ \vdots \\ u_{N-2} \\ u_{N-1} \end{pmatrix} \quad (\text{A.14})$$

Appendix A. Numerical Approximations of the Eigenvalue Problem

$$D^3 \begin{pmatrix} u_2 \\ u_3 \\ u_4 \\ u_5 \\ \vdots \\ u_{N-2} \\ u_{N-1} \end{pmatrix} = \frac{1}{h^3} \begin{pmatrix} -\frac{1}{2} & -1 & \frac{1}{2} & 0 & 0 & 0 & \cdots & 0 \\ 1 & 0 & -1 & \frac{1}{2} & 0 & 0 & \cdots & 0 \\ -\frac{1}{2} & 1 & 0 & -1 & \frac{1}{2} & 0 & \cdots & 0 \\ 0 & -\frac{1}{2} & 1 & 0 & -1 & \frac{1}{2} & \cdots & 0 \\ & & \ddots & & & & \ddots & \\ 0 & 0 & \cdots & -\frac{1}{2} & 1 & 0 & -1 & \frac{1}{2} \\ 0 & 0 & \cdots & 0 & -\frac{1}{2} & 1 & 0 & -1 \\ 0 & 0 & \cdots & 0 & 0 & -\frac{1}{2} & 1 & \frac{1}{2} \end{pmatrix} \begin{pmatrix} u_2 \\ u_3 \\ u_4 \\ u_5 \\ \vdots \\ u_{N-2} \\ u_{N-1} \end{pmatrix} \quad (\text{A.15})$$

$$D^4 \begin{pmatrix} u_2 \\ u_3 \\ u_4 \\ u_5 \\ \vdots \\ u_{N-2} \\ u_{N-1} \end{pmatrix} = \frac{1}{h^4} \begin{pmatrix} 7 & -4 & 1 & 0 & 0 & 0 & \cdots & 0 \\ -4 & 6 & -4 & 1 & 0 & 0 & \cdots & 0 \\ 1 & -4 & 6 & -4 & 1 & 0 & \cdots & 0 \\ 0 & 1 & -4 & 6 & -4 & 1 & \cdots & 0 \\ & & \ddots & & & & \ddots & \\ 0 & 0 & \cdots & 1 & -4 & 6 & -4 & 1 \\ 0 & 0 & \cdots & 0 & 1 & -4 & 6 & -4 \\ 0 & 0 & \cdots & 0 & 0 & 1 & -4 & 7 \end{pmatrix} \begin{pmatrix} u_2 \\ u_3 \\ u_4 \\ u_5 \\ \vdots \\ u_{N-2} \\ u_{N-1} \end{pmatrix} \quad (\text{A.16})$$

Note that for the eigenfunction  $v$  we will only require the first and second derivative matrices, and according to the boundary conditions (A.5) - (A.8) these will be the same ones as those that are used for  $u$ .